Nonlinear Dynamics (2026)114:1142
https://doi.org/10.1007/s11071-026-12970-2

RESEARCH

Experimental modal analysis of nonlinear systems using force-controlled harmonic testing

M. Fatih Gürbüz[1,2] · M. Bülent Özer[2] · H. Nevzat Özgüven[2]

Received: 13 January 2026 / Revised: 11 August 2026 / Accepted: 12 August 2026
© The Author(s) 2026

Abstract

This paper presents the Force-Controlled Testing-Harmonic Force Surface (FCT-HFS) framework, a novel approach for experimental modal analysis that identifies nonlinear modal models using standard force-controlled testing. Based on single nonlinear normal mode theory and quasi-linearisation in experimental analysis of nonlinear systems, the framework represents nonlinearities as response-amplitude-dependent modal parameters. The framework involves conducting a series of force-controlled frequency response tests to construct a three-dimensional HFS. By slicing this surface at constant response amplitude planes, quasi-linear frequency response functions (FRFs) are extracted, allowing the identification of amplitude-dependent modal parameters through established linear modal identification techniques. The proposed framework is validated through numerical simulations and experimental investigations of two benchmark structures: the length-modified Brake-Reuß beam and the Orion beam. It is observed that the accuracy of synthesised responses is highly sensitive to the density of forcing levels and to the interpolation techniques employed during both HFS construction and modal-parameter curve fitting. Numerical and experimental results demonstrate that the proposed framework accurately captures the nonlinear modal model of nonlinear systems, provided that no unstable branch exists in the frequency response. Consequently, the framework is well-suited for weakly nonlinear systems and systems with strong nonlinear damping where a jump does not occur. The FCT-HFS framework eliminates the need to measure quasi-linear FRFs through response-controlled testing using specialised control systems, enabling the use of well-established force-controlled harmonic testing methods and equipment while still capturing the key benefits of the response-controlled nonlinear modal analysis approach when there is no unstable branch in the frequency response.

✉ M. Fatih Gürbüz
mfg35@cam.ac.uk

[1] Department of Engineering, University of Cambridge, Cambridge, UK

[2] Department of Mechanical Engineering, Middle East Technical University, Ankara, Türkiye

Published online: 09 September 2026

Graphical abstract

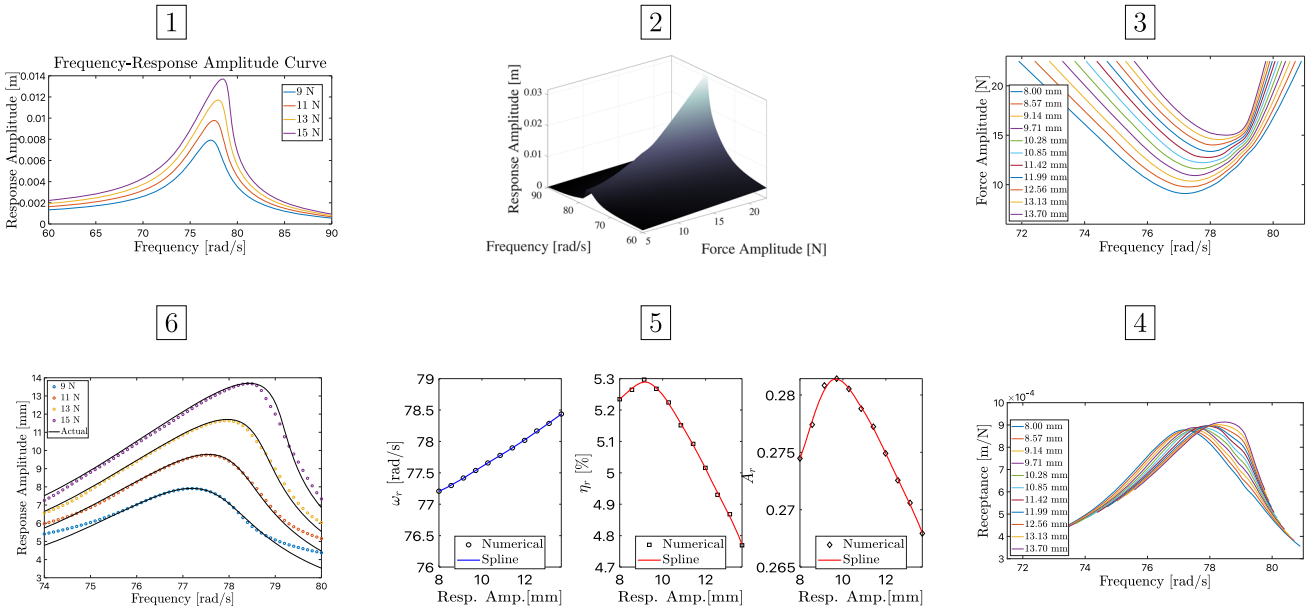

Keywords Nonlinear system identification · Nonlinear normal mode · Harmonic force surface · Force-controlled testing · Nonlinear experimental modal analysis

1 Introduction

Humanity has long endeavoured to create and optimise machines and structures that meet societal requirements. Engineers across different disciplines design and analyse these systems to ensure both safety and optimal performance. System identification methods [1] are used to find the parameters of a mathematical model that links the inputs to the outputs of these systems. For many decades, linear system identification frameworks have been developed and refined, proving immensely valuable for the analysis of structures and machines. Nonetheless, most real-world applications exhibit varying degrees of nonlinearity arising from many factors. Furthermore, as the complexity of the structures increases, the inherent limitations of linear system identification techniques have become increasingly evident, particularly in structural dynamics, where nonlinearities such as friction and large deformations are significant. These limitations lead to significant inaccuracies in conventional linear modal analysis and identification techniques. Recognising these challenges, remarkable progress has been made in nonlinear system identification over the past two decades, and a systematic introduction to parameter identification has been presented [2, 3]. Nonetheless, numerous challenges remain.

The pioneering work by Rosenberg [4–6] in the 1960s introduced the nonlinear normal mode (NNM), a benchmark for modal methods in nonlinear system identification. Subsequent work by Szemplinska-Stupnicka [7, 8] in 1979 and 1983 showed that a single nonlinear normal mode (SNNM) can represent the response of a nonlinear system around resonance, provided that the modes are well separated and no modal coupling occurs at the relevant energy level. The frequency response functions (FRFs) can thus be represented using a single nonlinear normal mode and its natural frequency. This concept guided many works in the community; for instance, in the early 1980s, Jézéquel [9] utilised the SNNM theory to analyse bolted joints under harmonic oscillations using the Krylov–Bogoliubov linearisation method, validated on circular plates. Later, Setio et al. [10] identified modal parameters in Duffing's oscillator by utilising the minimisation between the force-controlled sweep sine testing frequency response curves and analytical ones from NNMs in the early 1990s, with validation on a beam exhibiting local nonlinear stiffness.

Over time, these foundational methods were extended to cover linear and nonlinear friction damping, widely

applicable in blade vibration studies by Chong and Imregun [11]. In 2002, Gibert [12] presented a similar approach to Setio et al. to identify the modal parameters by minimising the error between the theoretical and experimental receptance. Later, a nonlinear resonant decay method based on NNMs was proposed. The method was validated using a 5-degree-of-freedom (DOF) system and a nonlinear panel structure [13], a wing/pylon/store experimental setup [14], and real aeroplane test data [15]. Özer et al. [16] in 2009 employed the describing function technique to detect and characterise nonlinearity in multi-degree-of-freedom (MDOF) systems. The approach is applicable to cases where there exists a single nonlinear element in the system. Subsequently, Aykan and Özgüven [17] made improvements to the method developed to address this limitation. Ahmadian et al. [18] identified the modal parameters of a beam with frictional contact support, using both the SNNM approach and the restoring force surface (RFS) method, a time domain method developed by Masri and Caughey [19]. Beyond NNM-based methods, several other valuable approaches have been introduced in the literature. In the context of linearization methods, Wang and Zheng [20] developed the equivalent dynamic stiffness mapping technique, validated on a metal mesh damper. Furthermore, other studies employed time-varying models, utilising small time increments for linear identification. Sracic and Allen [21] published interesting research using linear time-periodic approximations. Regarding frequency domain methods, Noël and Kerschen [22] applied their nonlinear subspace identification method to the benchmark for nonlinear structural identification (BENSI) developed by Carri and Ewins [23]. Recently, Kwarta and Allen [24] introduced a nonlinear system identification technique called nonlinear identification through extended outputs (NIXO), which extends NIFO (nonlinear identification through feedback of the outputs) developed by Adams and Allemang [25]. Unlike NIFO, NIXO provides a single value for the nonlinear modal parameters, whereas the modal parameters vary depending on the frequency in the NIFO method.

In recent years, the structural vibrations community has developed novel techniques to reduce the experimental complexity and effort for applications in both industry and academia. To this end, direct parameter estimation methods have become popular over the past decade. For instance, Renson et al. [26] proposed a robust method (control-based continuation, CBC) to extract the backbone curve of the nonlinear systems and compared it with the resonant-decay method. A single-DOF oscillator with base excitation was used with a single point, one harmonic, to validate the method. It was demonstrated that CBC successfully overcame the challenges posed by bifurcations and stability changes that could affect the system. Furthermore, Peter and Leine [27] presented the phase-locked-loop (PLL) method. They introduced an innovative nonlinear mode indicator function based on power, which is simple to implement. The PLL controller automatically tunes the excitation phase, leading to substantial time savings with this closed-loop controller. To validate its effectiveness, the methodology was tested on a clamped steel beam, demonstrating faster and more robust tracking of the backbone curve compared to other controllers. More recently, Karaağaçlı and Özgüven [28] generalised the response-controlled testing method proposed [29, 30] for systems with nonlinear elements between a single coordinate and ground to systems with many and even distributed nonlinear elements. The response-controlled stepped sine testing (RCT) method obtains a modal model of a nonlinear system by identifying response-dependent modal parameters of a nonlinear system from measured quasi-linear FRFs. The method was successfully applied to a real missile [28], a geometrically nonlinear structure [31, 32], to a stack-type piezoelectric actuator mechanism [33], a control fin actuator mechanism [34, 35] that exhibits high stiffness and high damping nonlinearity, and the benchmark system of the TRChallenge [36]. In a recent work, Di Maio [37] proposed a modified-Dobsen method for extracting nonlinear modal parameters.

Building on advancements in measuring and using quasilinear FRFs, this paper proposes a novel approach for identifying amplitude-dependent modal parameters from the classical Force-Controlled Testing (FCT) conducted at different force levels. After constructing a Harmonic Force Surface (HFS) [38] from these measured force-controlled FRFs, quasi-linear FRFs are extracted without requiring response-controlled testing. Thus, in this study, the RCT-HFS framework is replaced by the so-called FCT-HFS framework. As in the RCT-HFS, this approach is also based on the single NNM theory and assumes that a harmonically excited nonlinear system vibrates harmonically at the same frequency, i.e., higher harmonics are negligible, and there is no internal resonance. These assumptions are also used in similar studies and are valid for a wide range of nonlinear structures. However, the FCT-HFS approach has a further limitation: it can be applied to nonlinear systems where there is no jump in the measured frequency response. FCT may yield poor estimates of the true dynamic behaviour in nonlinear systems exhibiting jump phenomena and unstable response branches; otherwise, the FCT measurement strategy is less demanding than RCT, especially if the Siemens Testlab data acquisition system is not available. Moreover, a single force-controlled frequency sweep is sufficient to obtain the frequency response at a single harmonic forcing level, whereas reconstructing the same frequency response using RCT requires several response-controlled sweeps

performed at different prescribed response-amplitude levels. Under these conditions, the FCT-HFS approach makes use of more easily measured force-controlled frequency response curves to create the HFS. Then, quasi-linear frequency response curves are obtained from the HFS, and the modal parameters at each displacement level are identified by employing any linear modal identification technique. Thus, a modal model of the nonlinear system is obtained, which can be used to calculate the synthesised frequency response for any given harmonic forcing. It should be noted that the HFS concept was originally developed to obtain more accurate frequency response measurements of nonlinear systems, including unstable branches, if there are any. In contrast, within the FCT-HFS framework, HFS is employed to identify response-dependent modal parameters of nonlinear systems. The measured and synthesised frequency response curves are compared to evaluate the accuracy of the proposed approach.

Alternatively, fixed-voltage frequency sweeping provides an open-loop experimental approach in which shaker voltage is held constant during each frequency sweep, and the sweep is repeated at several prescribed voltage levels [39]. A related but distinct technique is fixed-frequency voltage control testing (FFVCT), in which the excitation frequency is held fixed while the voltage supplied to the electrodynamic shaker is varied and the applied force and structural response are measured. By exploiting force drop-out and the coupled shaker-structure dynamics, FFVCT has been used to recover multivalued force-response curves without closed-loop force or response control [39] and to reconstruct constant-response FRFs for nonlinear parameter identification [40]. However, its ability to stabilise and trace unstable response branches depends on the shaker properties, shaker-structure coupling, and excitation location [41].

The present study significantly extends the previous work reported in [42], while also benefiting from the subsequent developments and additional investigations presented in the thesis of Gürbüz [43], which contributed to a deeper understanding of the working principles, capabilities, and limitations of the FCT-HFS framework. In particular, the present study systematically investigates both the strengths and limitations of the method through additional analyses. These include the effect of the forcing levels used for HFS generation on FRF prediction accuracy, as well as the influence of curve fitting techniques employed for modal parameter estimation. Furthermore, the study examines how the approach can be applied to nonlinear systems when the available quasi-linear FRFs are incomplete, either due to jump phenomena or missing data points associated with untested response levels. In addition, the applicability of the framework is demonstrated more concretely through additional benchmark case studies. It is expected that the method can be used widely in academia and industry.

The rest of the paper is organised as follows. In Sect. 2, the theoretical framework of the proposed method is given. Section 3 presents numerical validation and verification of the proposed method. In Sect. 4, the experimental applications of the proposed method are presented. Finally, Sect. 5 provides the results and conclusions.

2 Theory

2.1 Modal analysis of nonlinear systems using the single nonlinear normal mode (SNNM) theory

Consider a nonlinear MDOF system with structural damping subjected to harmonic excitation at an excitation frequency ω. For a steady-state harmonic response, neglecting higher harmonics, the governing equation in the frequency domain is

$$\left(-\omega^2\boldsymbol{M} + i\boldsymbol{H} + \boldsymbol{K}\right)\boldsymbol{X} + \boldsymbol{F}_N = \boldsymbol{F} \tag{1}$$

where $\boldsymbol{M}, \boldsymbol{H}$, and $\boldsymbol{K}$ are the mass, hysteretic damping and stiffness matrices, respectively. $\boldsymbol{X}$ is the steady-state displacement amplitude, and $\boldsymbol{F}_N$ and $\boldsymbol{F}$ are the amplitudes of the nonlinear internal and external forces, respectively. Here, i represents the unit imaginary number. Furthermore, according to the Describing Function Method (DFM) [44], the amplitude of the nonlinear internal force $\boldsymbol{F}_N$ can be expressed as

$$\boldsymbol{F}_N = \boldsymbol{\Delta}\boldsymbol{X} \tag{2}$$

where $\boldsymbol{\Delta}$ is the displacement amplitude-dependent *nonlinearity matrix*. Thus, Eq. (1) can be written as

$$\left(-\omega^2\boldsymbol{M} + i\boldsymbol{H} + \boldsymbol{K} + \boldsymbol{\Delta}_{re} + i\boldsymbol{\Delta}_{im}\right)\boldsymbol{X} = \boldsymbol{F} \tag{3}$$

where $\boldsymbol{\Delta}_{re}$ and $\boldsymbol{\Delta}_{im}$ denote the real and imaginary parts of the nonlinearity matrix, representing equivalent stiffness and damping matrices for displacement amplitude $\boldsymbol{X}$, respectively, associated with the nonlinearity in the system. This equation represents the quasi-linearisation of a nonlinear system, a concept that was proposed first in the 1990s [44, 45]. Quasi-linearisation represents nonlinear elements with response-amplitude-dependent linear elements, so that for a fixed response amplitude level, the nonlinear system behaves linearly.

According to the SNNM theory [7], for a system with well-separated modes and no internal resonance, the solution of Eq. (3) around the r th resonance frequency can be written as

$$\boldsymbol{X} = \widetilde{q}_r \boldsymbol{\phi}(q_r)_r \tag{4}$$

where $\widetilde{q}_r$ is the rth modal displacement response, q_r is the amplitude of $\widetilde{q}_r$, and $\boldsymbol{\phi}(q_r)_r$ is the rth nonlinear normal mode that can be calculated from the following eigenvalue problem

$$(\boldsymbol{K} + \boldsymbol{\Delta}_{re})\boldsymbol{\phi}(q_r)_r = \omega_r^2(q_r)\boldsymbol{M}\boldsymbol{\phi}(q_r)_r \tag{5}$$

Note that the solution of the above eigenvalue problem yields real eigenvectors as $\boldsymbol{\Delta}_{re}$ is a symmetric matrix [44], and the solution requires iteration as the nonlinearity matrix is a function of response level, and that is extremely expensive for finite element models of real structural systems. However, this formulation is presented here just to give the theoretical base; otherwise, for analytical analysis of nonlinear structures under harmonic excitation, methods that reduce computational effort drastically can be employed [44, 46, 47]. Inserting Eq. (4) into Eq. (3), premultiplying by $\boldsymbol{\phi}(q_r)_r^T$, and then arranging it gives

$$\left(-\omega^2 m_r(q_r) + i h_r(q_r) + k_r(q_r)\right)\widetilde{q}_r = \boldsymbol{\phi}(q_r)_r^T \boldsymbol{F} \tag{6}$$

where $m_r(q_r) = \boldsymbol{\phi}(q_r)_r^T \boldsymbol{M}\boldsymbol{\phi}(q_r)_r$, $k_r(q_r) = \boldsymbol{\phi}(q_r)_r^T (\boldsymbol{K} + \boldsymbol{\Delta}_{re})\boldsymbol{\phi}(q_r)_r$, and $h_r(q_r) = \boldsymbol{\phi}(q_r)_r^T (\boldsymbol{H} + \boldsymbol{\Delta}_{im})\boldsymbol{\phi}(q_r)_r$ are modal mass, modal stiffness, and modal damping, respectively. Modal response amplitude, $\widetilde{q}_r$, can be calculated from Eq. (7) as

$$\widetilde{q}_r = \frac{\boldsymbol{\phi}(q_r)_r^T \boldsymbol{F}}{m_r(q_r)\left(-\omega^2 + i\eta_r(q_r)\omega_r^2(q_r) + \omega_r^2(q_r)\right)} \tag{7}$$

where

$$\omega_r(q_r) = \left(k_r(q_r)/m_r(q_r)\right)^{1/2}$$

and $\eta_r(q_r) = h_r(q_r)/(k_r(q_r))$ are the rth natural frequency and rth modal damping ratio, respectively. Consequently, the amplitude of the near-resonant response at the rth mode can be obtained from Eq. (4) as follows

$$\boldsymbol{X} = \frac{\boldsymbol{\phi}(q_r)_r \boldsymbol{\phi}(q_r)_r^T \boldsymbol{F}}{m_r(q_r)\left(-\omega^2 + i\eta_r(q_r)\omega_r^2(q_r) + \omega_r^2(q_r)\right)} \tag{8}$$

which can also be written in terms of mass-normalized nonlinear normal mode

$$\overline{\boldsymbol{\phi}}(q_r)_r = \boldsymbol{\phi}(q_r)_r / \sqrt{m_r(q_r)} \tag{9}$$

as

$$\boldsymbol{X} = \frac{\overline{\boldsymbol{\phi}}(q_r)_r \overline{\boldsymbol{\phi}}(q_r)_r^T \boldsymbol{F}}{\left(-\omega^2 + i\eta_r(q_r)\omega_r^2(q_r) + \omega_r^2(q_r)\right)} \tag{10}$$

Then, the receptance for a jth coordinate when a force is applied at a kth coordinate can be written as

$$\alpha_{jk}(\omega, q_r) = \frac{\overline{\phi}_{jr}(q_r)\overline{\phi}_{kr}(q_r)}{\left(-\omega^2 + i\eta_r(q_r)\omega_r^2(q_r) + \omega_r^2(q_r)\right)} \tag{11}$$

which can be written as

$$\alpha_{jk}(\omega, q_r) = \frac{A_{jkr}(q_r)}{\left(-\omega^2 + i\eta_r(q_r)\omega_r^2(q_r) + \omega_r^2(q_r)\right)} \tag{12}$$

where $A_{jkr}(q_r)$ is defined as the modal constant.

The proposed framework can also be applied to viscously damped systems. For such a system, the corresponding frequency-domain equation is

$$\left(-\omega^2 \boldsymbol{M} + i\omega \boldsymbol{C} + \boldsymbol{K}\right)\boldsymbol{X} + \boldsymbol{F}_N = \boldsymbol{F} \tag{13}$$

where $\boldsymbol{C}$ is the viscous damping matrix. Following similar steps, the receptance expression can be obtained as

$$\alpha_{jk}(\omega, q_r) = \frac{A_{jkr}(q_r)}{\left(-\omega^2 + i2\zeta_r(q_r)\omega\omega_r(q_r) + \omega_r^2(q_r)\right)} \tag{14}$$

where $c_r(q_r) = \boldsymbol{\phi}(q_r)_r^T (\boldsymbol{C} + \boldsymbol{\Delta}_{im})\boldsymbol{\phi}(q_r)_r$ is the response-amplitude-dependent modal damping, and $\zeta_r(q_r) = \frac{c_r(q_r)}{2m_r(q_r)\omega_r(q_r)}$ is the corresponding modal damping ratio.

2.2 Experimental modal analysis of nonlinear systems using quasi-linearization through response-controlled testing: RCT-HFS framework

In this section, brief information is given about response-controlled testing, which will make it easier to follow the FCT-HFS framework proposed. Response-controlled testing for experimental modal analysis of a nonlinear system was first proposed by Arslan and Özgüven [29, 30] for systems with local grounded nonlinearity. Later, it is generalised to systems with distributed nonlinearity, and the RCT method proposed [28] has been successfully applied to several benchmarks and industrial systems [28, 29, 31–33]. The response-controlled testing approach is, in a way, an experimental equivalent of the nonlinearity matrix concept used in analytical nonlinear analysis and represents quasi-linearisation in experimental nonlinear analysis. The quasi-linearisation property is a fundamental concept employed in both RCT-HFS and FCT-HFS frameworks. As can be seen from Eqs. (12) and (14), if the amplitude of the rth modal response, q_r, is kept fixed in a stepped-sine test at a near-resonant frequency, the nonlinear system is quasi-linearised, that is, the system will behave linearly.

From Eq. (4), it can be concluded that by keeping the amplitude of the modal response, q_r fixed, for cases where the system is excited at a single point near resonance, the displacement amplitude vector of the system remains fixed.

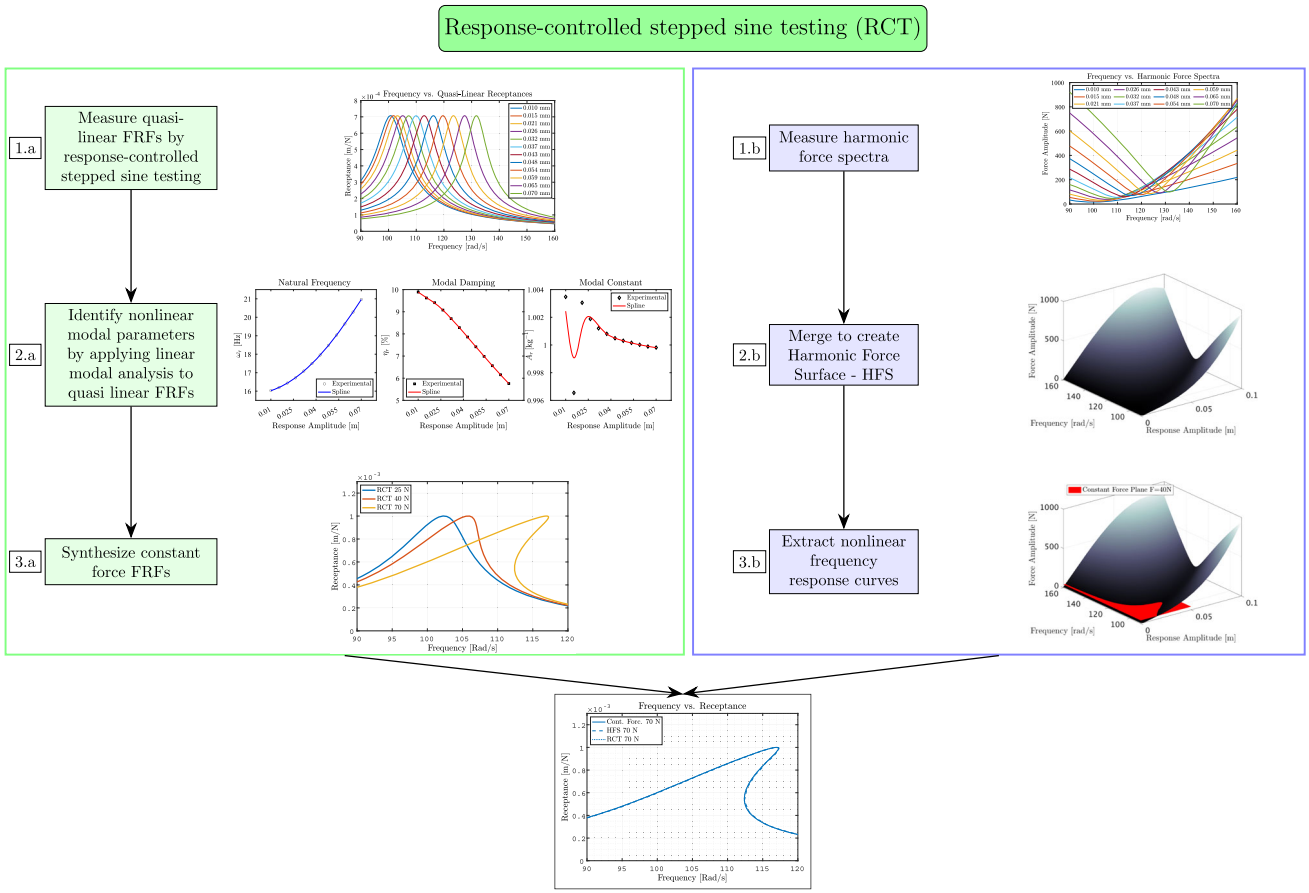

Fig. 1 Flowchart for Procedure of RCT-HFS Framework

RCT is applied by keeping the response amplitude of any selected point on the system (usually the excitation point) fixed, which ensures that the amplitudes of all coordinates are kept fixed. The RCT-HFS framework is outlined in Fig. 1. The process comprises two distinct paths, RCT and HFS: RCT is the experimental modal analysis path followed for the modal identification of nonlinearity, which yields the modal model of the nonlinear system that can be used to synthesise the harmonic response of the system for a given harmonic forcing, provided that higher harmonics do not contribute and there is no internal resonance. A brief description of RCT is summarised in Fig. 1 (first column).

The right branch describes the construction of HFS [28], which is basically a surface composed of nonlinear frequency response curves, each corresponding to a different excitation force amplitude. However, the surface is not constructed by combining various nonlinear frequency response curves; on the contrary, it is used to obtain nonlinear frequency responses for different forcing amplitudes. The construction of HFS is explained below (refer to Fig. 1, second column).

Step 1.b: Harmonic force spectra within the frequency range are measured through RCT by keeping the harmonic response amplitude of the driving point at a fixed level.

Step 2.b: These spectra are merged to construct a continuous HFS by linear interpolation, with frequency and response amplitude as the independent variables and force amplitude as the dependent variable.

Step 3.b: Nonlinear frequency response curves for the required forcing levels are extracted by slicing the HFS at these force amplitude levels. Note that the frequency responses obtained from HFS are derived from the reconstruction of purely experimental data, and interestingly, these curves give the experimentally measured frequency responses at even unstable branches.

Obtaining two different frequency–response curves using the RCT-HFS framework from the same measurement data set, but in two different ways (either by extracting them from the HFS, which are purely measured values, or by synthesising them from the identified nonlinear modal parameters), provides self-validation of the

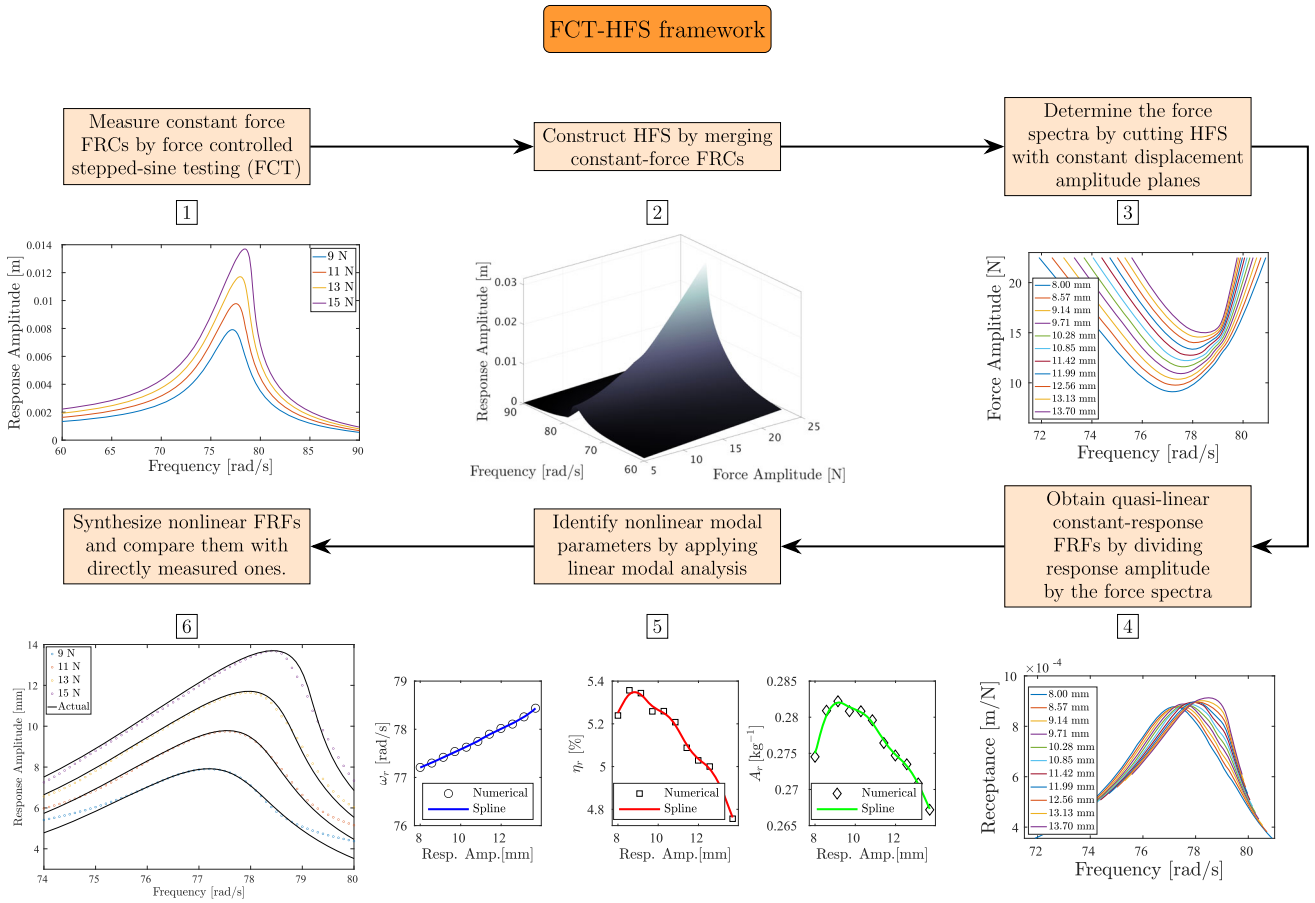

Fig. 2 Flowchart for the FCT-HFS framework- experimental nonlinear system identification

RCT method used for the experimental modal analysis of nonlinear systems.

2.3 Using harmonic force surface to obtain quasi-linear FRFs from measured nonlinear FRFs: FCT-HFS framework

The aim in constructing the HFS using measured quasi-linear FRFs was to extract measured nonlinear frequency response curves by slicing the HFS at fixed force amplitude levels. However, as a novel approach, it is proposed [42, 43] to construct it by combining nonlinear frequency response curves measured at various forcing amplitudes, and slice it at fixed response amplitudes to obtain quasi-linear FRFs from which nonlinear modal identification can be made. The FCT-HFS framework is summarised in Fig. 2:

Step 1: Nonlinear frequency responses are measured by using classical force-controlled stepped-sine tests for various force amplitude values around a resonance.

Step 2: Using the measured nonlinear frequency response curves, the harmonic force surface is constructed in a three-dimensional space of frequency, force and displacement.

Step 3: The measured data are linearly interpolated to construct a continuous HFS, with frequency and force amplitude as the independent variables and response amplitude as the dependent variable. Subsequently, harmonic force spectra for several different displacement levels are obtained by cutting HFS with constant displacement amplitude planes. The number of constant displacement planes used and the differences between each are important to increase the accuracy.

Step 4: Quasi-linear FRFs are then calculated by dividing constant response amplitudes by the corresponding forces at each frequency.

Step 5: Linear modal identification techniques are applied to the quasi-linear FRFs to estimate the response-dependent modal parameters. Identified modal parameters constitute the modal model of the nonlinear system.

Step 6: The identified modal model can then be used to synthesise the nonlinear response curves for a given forcing level.

To perform the synthesis after the modal model is constructed, the nonlinear response is typically calculated using the arclength continuation method coupled with Newton's method. At this stage, the need for a closed-form expression for the modal parameters becomes evident. The proposed method performs well when the extracted response amplitude levels lie within the range covered by the available data. However, when predictions are required outside this range, additional treatments may be necessary, as discussed in a subsequent section. Furthermore, since the solution procedure is inherently iterative, the modal parameters are response dependent. Alternatively, a recent, straightforward approach [48] can be applied to obtain the response by using the response-dependent modal model without iteration. In this approach, the SNNM formulation is employed, and a closed-form equation is solved directly for the excitation frequencies corresponding to a given response level. Thus, an unstable branch, if it exists, can also be captured as the solution yields two frequencies at a given modal amplitude. Note that the response for the forcing levels at which experiments are conducted can be synthesised for self-validation of the modal model obtained. Further details of the above steps will be provided in the subsequent sections, with emphasis on the points that should be noted to enhance the identification process.

3 Numerical validation and verification of the FCT-HFS method

In this section, numerical applications of the proposed method will be conducted to validate its applicability and efficacy. Specifically, a polynomial type of stiffness is utilised as the nonlinear element in the analysed systems, allowing for the evaluation of the method's performance under conditions representative of practical nonlinear scenarios. All numerical systems examined here are simulated under harmonic forcing conditions. Throughout these analyses, the single harmonic DFM is utilised [44]. To further clarify these findings and critically evaluate the performance of the method, comparative analyses are performed to understand the sensitivities and the limitations inherent in the proposed method.

Table 1 Values of the system parameter for the 3-DOF system

m [kg]	k [N/m]	h [N/m]	k_c [N/m^3]
1	1e4	5e2	1e7

3.1 Case study 1: three-DOF system with cubic stiffness nonlinearity

Consider a 3 DOF system exhibiting cubic nonlinearity, as depicted in Fig. 3. The first degree of freedom is subjected to a harmonic forcing with an amplitude of f, each DOF has a mass m, and they are connected with springs with stiffness, k, and structural damping elements with a coefficient h. The cubic stiffnesses are positioned between every DOF except the ground and the first DOF. The nonlinear internal force associated with the cubic stiffness can be expressed as follows:

$$n(y) = k_c y^3 \tag{15}$$

where y represents the relative displacement of the cubic stiffness. Without delving into the derivations, the describing function of a cubic stiffness can be expressed as follows:

$$v = \frac{3}{4} k_c Y^2 \tag{16}$$

where Y is the relative displacement amplitude that cubic stiffness experiences.

The numerical values used in this case study are given in Table 1.

Firstly, constant force frequency response curves (FRCs) are determined at forcing levels of 9, 11, 13, and 15 N using Eq. (3) and employing the arclength continuation algorithm in the range of 60 to 90 rad/s as shown in Fig. 4a. Then, these FRCs are taken as simulated experimental results, and the forcing amplitude axis is added as a third axis, enabling the visualisation of these FRCs in a three-dimensional space, as depicted in Fig. 4b. The HFS is

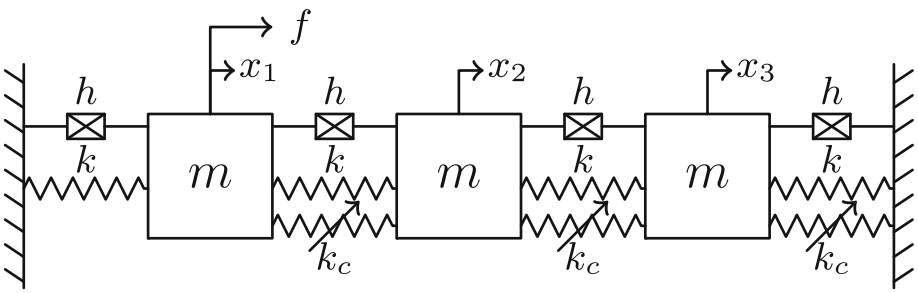

Fig. 3. 3 DOF discrete system

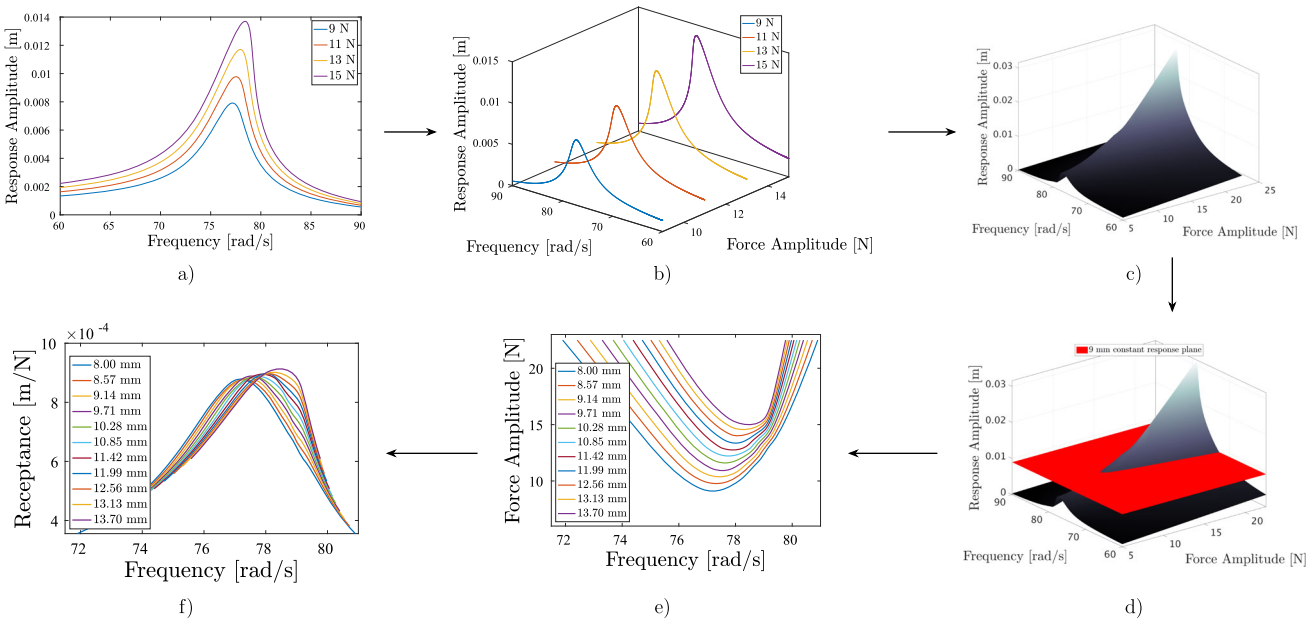

Fig. 4 The procedure summary for case study 1. **a** Measured FRFs **b** FRFs on 3D space **c** Constructed HFS **d** Extracting harmonic force spectra from the HFS **e** Harmonic force spectra on frequency-force amplitude plane **f** Quasi-linear FRFs for modal parameter identification

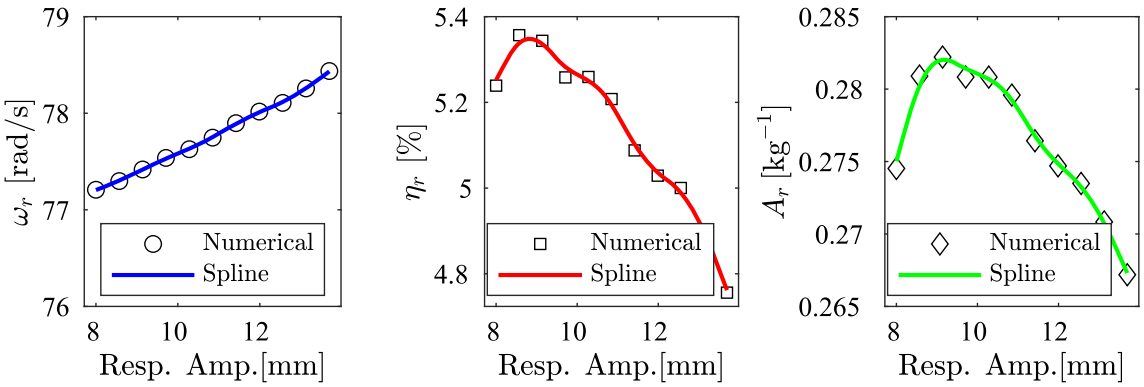

Fig. 5 Modal parameters obtained for case study 1

created using linear interpolation between the FRCs as illustrated in Fig. 4c. This process ensures the generation of a continuous surface, which is subsequently utilised to extract quasi-linear FRFs. Here, it is assumed that response amplitude varies linearly between the selected forcing amplitude levels. The HFS is intersected by constant response amplitude planes. This is performed systematically at multiple levels to ensure comprehensive coverage of the measured data. In consideration of brevity and clarity within the scope of this paper, only the constant response amplitude plane corresponding to a response of 9 mm is explicitly depicted in Fig. 4d. Figure 4e shows the force spectra extracted for a total of 11 distinct response amplitude levels, ranging from low to high. Quasi-linear constant response FRFs are derived by dividing each constant response by the corresponding force spectra, as depicted in Fig. 4f. Using the quasi-linear FRFs for each constant response amplitude, the modal parameters can be calculated for each response amplitude. In this study, the simple peak picking method is used for modal parameter identification, and the identified and curve-fitted parameters are reported in Fig. 5. Note that the selected lower bound does not correspond to the minimum displacement at the lowest forcing level. This non-ideal choice is intentional and will be discussed further in Sect. 3.3.

Once modal parameters are identified and a modal model is obtained, frequency responses corresponding to given forcing amplitudes can be calculated, using the single NNM as

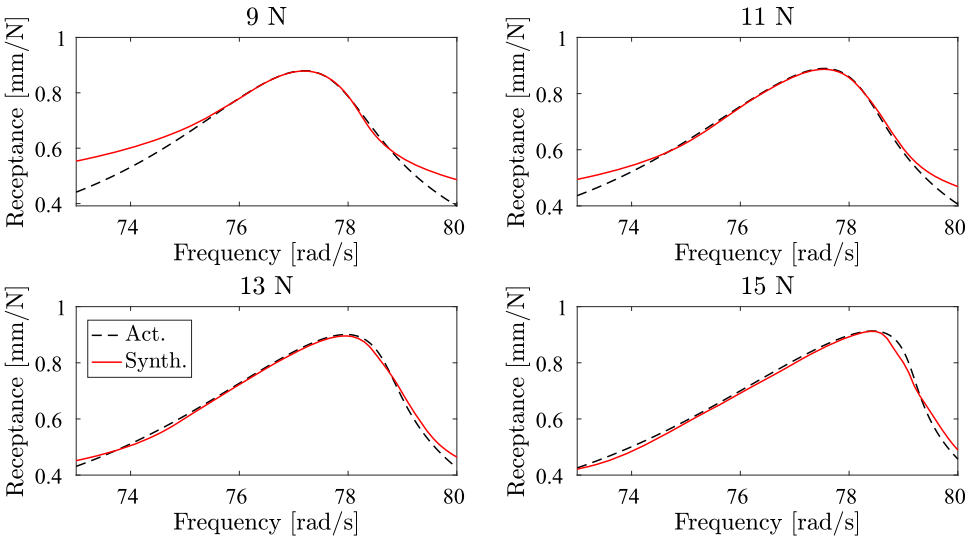

Fig. 6 FRFs comparison for case study 1

Table 2 Percentage norm error for case study 1

Forcing [N]	9	11	13	15
$\epsilon_{\%}$	6.84	3.24	1.94	2.41

$$X_j(q_r) = \frac{A_{jkr}(q_r)F_k}{\left(-\omega^2 + i\eta_r(q_r)\omega_r^2(q_r) + \omega_r^2(q_r)\right)} \tag{17}$$

Then, the constant force FRFs can be obtained by dividing the frequency responses by the associated force amplitudes. As the modal parameters are response level dependent, the frequency responses are calculated by using an iterative computation. Alternatively, the approach proposed in [48] can be employed, and thus iteration is avoided.

The synthesised FRFs are compared with their original counterparts for forcing levels of 9, 11, 13, and 15 N in Fig. 6. A high level of similarity is evident between the synthesised and original FRFs around resonance for each forcing amplitude level, with a small deviation around resonance for 13 and 15 N forcing levels. Conversely, the agreement between the curves weakens at the off-resonance regions, as expected. The divergence observed between the actual and synthesised curves in Fig. 6, particularly in the lower-amplitude off-resonance regions, can be attributed to two primary factors. First, the synthesis relies on the SNNM theory, which assumes that the dynamic response is dominated by a single mode near resonance. As the excitation frequency moves away from the resonance, the neglected contributions become increasingly significant, leading to theoretical deviations. Second, and more importantly, the synthesis algorithm requires continuous modal parameters across the entire amplitude range. Since the constant-amplitude quasi-linear FRFs are only available down to a certain minimum displacement level, synthesising the low-amplitude off-resonance tails requires evaluating the system below this threshold. Consequently, the solver is forced to extrapolate the modal parameters beyond the available data range, which directly contributes to the divergence observed in these regions.

Furthermore, to quantitatively assess the accuracy of the proposed method, a standard error metric is employed. Specifically, the relative L_2 error norm (normalised Euclidean error) between the original and the synthesised FRCs is calculated as

$$\epsilon_{\%} = \frac{\left|\left|x_{exact} - x_{synth}\right|\right|_2}{||x_{exact}||_2} \times 100 \tag{18}$$

The error calculated for this case study is tabulated in Table 2. As seen from the table, the closest agreement is observed at the forcing amplitude 13 N level, whereas the highest deviation is obtained at the 9 N level.

3.2 Case study 2: three-DOF system with cubic stiffness nonlinearity—higher forcing amplitudes

In the preceding section, a comprehensive analysis of the proposed method is presented in a step-by-step manner, and complete agreement between the numerically simulated and synthesised FRFs around the resonance frequency is demonstrated. However, despite possessing cubic stiffness, the system in the previous section does not exhibit an unstable branch in the frequency response for the force levels used. In this section, again, the system depicted in

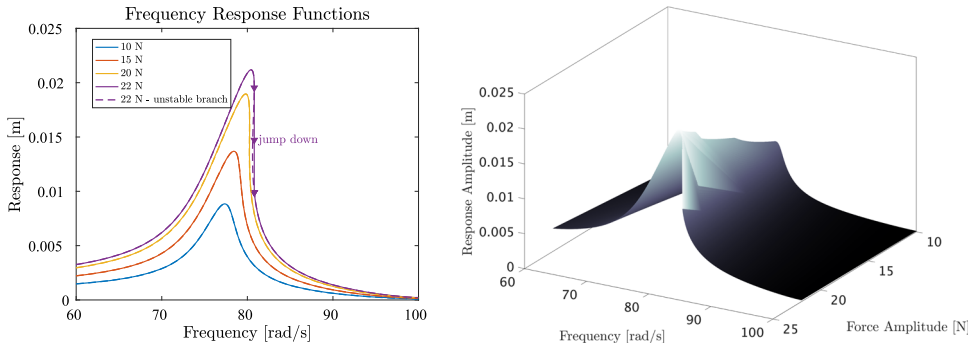

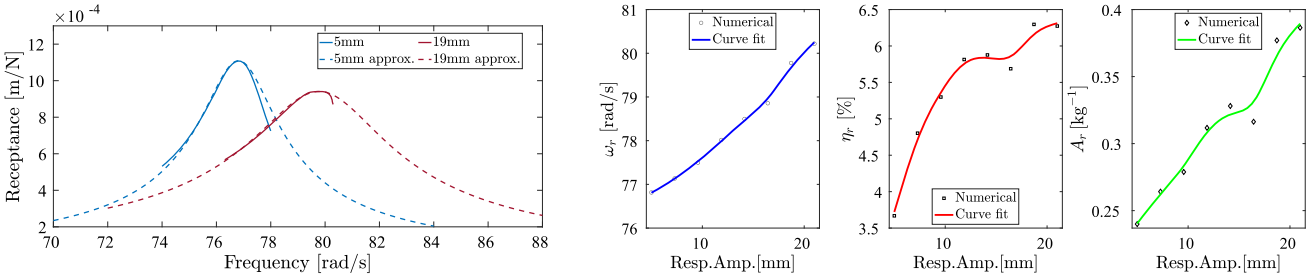

Fig. 8 **a** Comparison of some extracted and approximated quasi-linear FRFs **b** Modal Parameters for case study 2

Fig. 3 is utilised, but with higher excitations, which cause jumps in the frequency responses, to study the method's limitations. Figure 7a presents the frequency response curves for 10, 15, 20, and 22 N forcing amplitude levels. As shown in the figure, the frequency response curves for the lowest three forcing amplitude levels are without any unstable regions. Conversely, at a forcing amplitude of 22 Newtons, an unstable branch starts to emerge in the frequency response curve. The unstable branch obtained by arclength continuation is shown by the dashed line, whereas the solid downward-pointing arrows indicate the jump-down transition during an increasing-frequency

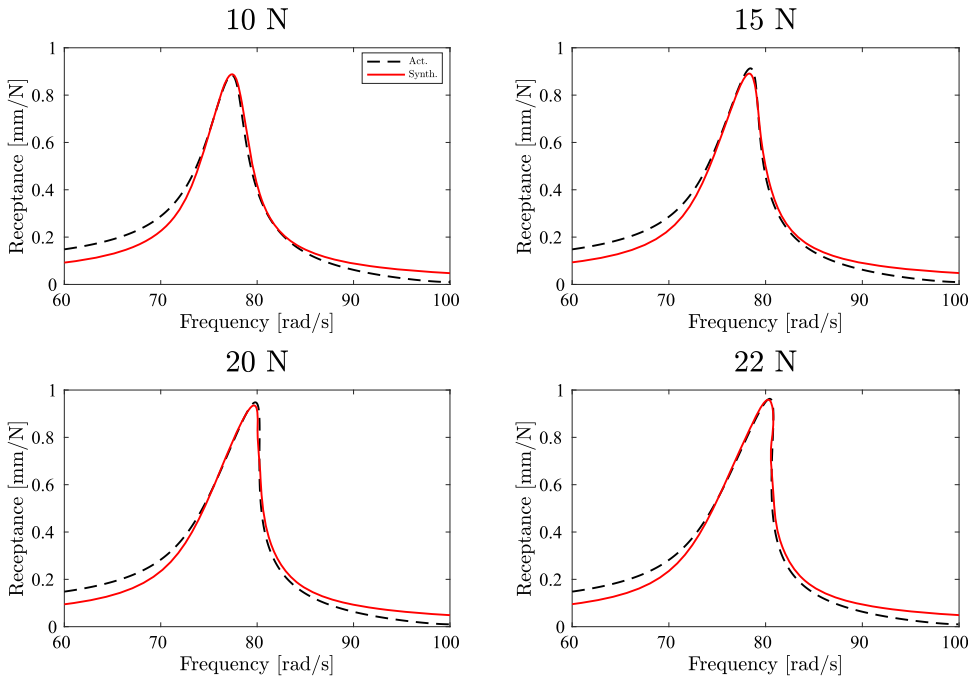

Fig. 9 Comparison of FRFs for case study 2

stepped-sine test. A potential limitation of the proposed method arises here, namely, a difficulty in constructing an HFS based on the frequency responses having unstable regions. The primary objective of the proposed method is to facilitate the transition from response-controlled tests to force-controlled harmonic response data for modal modelling of nonlinear systems. Ideally, an HFS constructed using quasi-linear FRFs obtained via RCT would fully capture the unstable branches of the FRCs. In contrast, when FCT is classically employed (as it is in the case of the proposed framework), the unstable branches cannot be physically measured. Consequently, the HFS constructed from FCT data is inherently incomplete, as it lacks the data corresponding to the unstable regime. In this section, we study the performance of the proposed approach for a forcing amplitude of 22 N, a forcing level at which the jump phenomenon starts to be observed. In this case, to address the above-mentioned fact, the HFS is constructed without considering the unstable region. Specifically, to represent a stepped-sine test with increasing frequency, the upper stable branch is retained up to the jump-down frequency, beyond which the lower stable branch is retained. The resulting FRC is therefore single-valued with respect to frequency, enabling interpolation between FRCs during construction of the HFS. It is easily seen that the HFS is not as continuous as in the previous example due to sharp changes in the FRCs.

Quasi-linear FRFs extracted from the HFS are presented in Fig. 8a for 5- and 19-mm levels with solid lines. As the response amplitude increases, the right-hand side of the extracted quasi-linear FRFs is distorted. As they do not present true quasi-linear FRFs, one cannot use these curves to determine the modal parameters, so here the second half-power point is approximated using the natural frequency and the lower half-power point frequency by simply assuming that the natural frequency is approximately equal to the mean of the two half-power point frequencies. The approximated parts of quasi-linear FRFs, after identifying modal parameters, are calculated using Eq. (17) and plotted on the same figure with dashed lines. The identified and curve-fitted cases are shown in Fig. 8b. Next, the original and synthesised FRFs are compared in Fig. 9. A satisfactory agreement is observed between the original and synthesised FRFs, particularly around the resonance frequency. However, when the force level increases further, so that the unstable region is more pronounced, it is observed that it is more difficult to apply the proposed method.

Table 3 Forcing levels used in Test 1, Test 2 and Test 3

Case	Forcing levels [N]
Test 1	9, 12, 15
Test 2	9, 11, 13, 15
Test 3	9, 9.5, 10, 10.5, 11, 11.5, 12 12.5, 13, 13.5, 14, 14.5, 15

3.3 Further considerations

In the first two subsections, the fundamental concepts of the FCT-HFS method are explained and applied to a three-degree-of-freedom system exhibiting cubic stiffness nonlinearity. This system is studied for various force levels, including ones causing unstable branches in its frequency responses. The results demonstrate that the proposed method performs with high efficacy in systems whose FRCs do not exhibit jump phenomena. The primary limitation, as identified in the previous section, arises from the occurrence of jumps in the FRC, which require careful consideration and appropriate use of the method. The subsequent sections provide further investigations on the method for enhancing its applicability. These include increasing the number of tests within the same force interval and employing various interpolating curve fitting techniques to the modal parameters identified.

3.3.1 Effect of conducting different numbers of force-controlled harmonic response data in identical intervals

HFS is constructed by interpolating between FRCs in a three-dimensional space. Consequently, the accuracy of the quasi-linear FRFs extracted from HFS is influenced by the number of force-controlled harmonic response data used within the same intervals. Table 3 presents three distinct test schemes to evaluate this effect. For brevity, the initial steps are omitted, starting directly with the modal parameter identification phase. In Test 1, a few constant force tests are performed at 3 discrete force amplitude levels. Test 2 utilises four discrete force amplitude levels. Test 3 is conducted at a highly dense grid of 13 discrete force amplitude levels within the same forcing interval. Figure 10a illustrates the modal parameters extracted from each corresponding HFS and their respective curve fits. To thoroughly examine the impact of varying the number of tests, identical curve-fitting procedures are applied to each scenario. Results indicate that the natural frequency values remain largely consistent across the three tests. However, noticeable discrepancies are observed in modal damping and modal constants at lower amplitude levels. The synthesised and original FRFs at 14 N forcing levels are compared in Fig. 10b. As evident from the comparison, conducting a higher number of force tests significantly enhances the accuracy of the synthesised FRFs. This

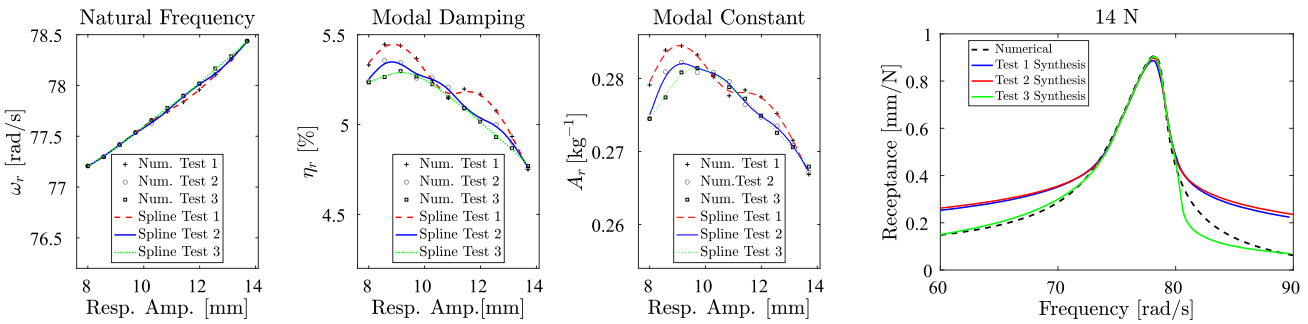

Fig. 10 Comparison of **a** Modal parameters, **b** FRFs for using different numbers of force-controlled harmonic response data within the same interval

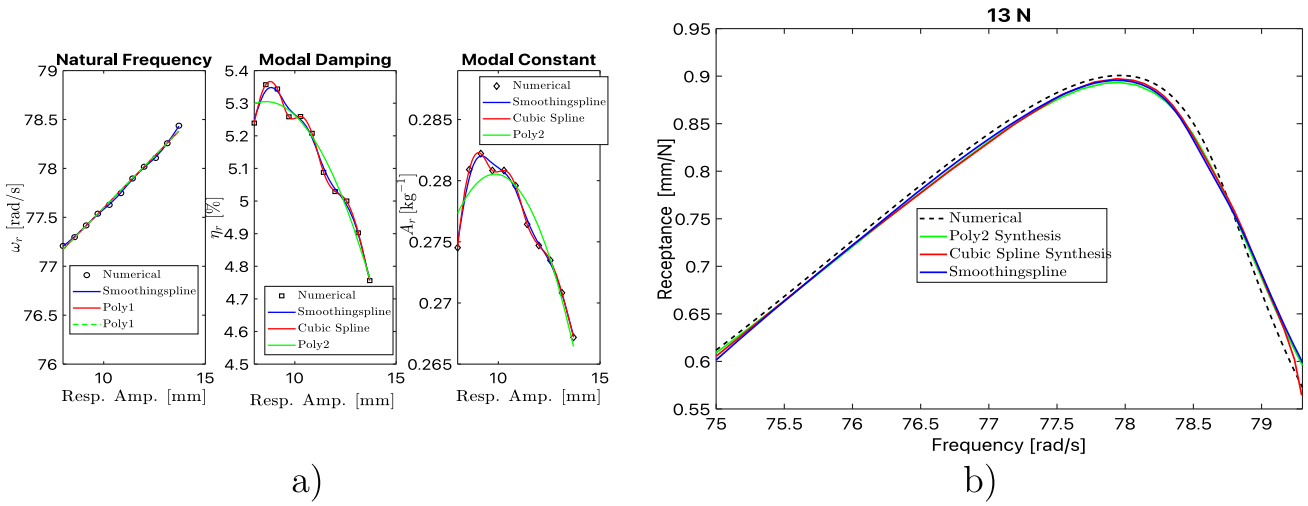

Fig. 11 Comparison of **a** different curve fits to the modal parameters, **b** FRF results using different curve fittings to the modal parameters

indicates that denser sampling primarily improves the stability of the reconstructed surface. While the improvement is most pronounced in the off-resonance regions, a noticeable enhancement is also observed near the resonance frequencies, where the predictions were already quite accurate. This improved accuracy is crucial in practical applications when precise behaviour of the system at off-resonance frequencies is important in our analyses and/or designs. It can therefore be concluded that selecting an appropriate number of forcing amplitude levels during the construction of the HFS is critical for ensuring accurate modal parameter extraction and subsequent synthesised FRF generation. Furthermore, the error analysis introduced in Eq. (18) gives 17%, 16% and 7% errors for Test 1, Test 2 and Test 3, respectively.

3.3.2 Curve fitting techniques for modal parameters

Another crucial aspect of the FCT-HFS method is the curve fitting to the identified modal parameters derived from the quasi-linear FRFs. The selection of the curve fitting technique for modal parameters holds significant importance, as these curve fits directly influence the accuracy and reliability of the subsequent synthesis process. Consequently, careful consideration and evaluation of different curve fitting techniques are essential to ensure valid and representative modal parameter estimates. Several different curve-fitting techniques are applied to investigate their impact on the derived modal parameters. The relationship between curve fitting and modal parameters is clearly illustrated in Fig. 11a, where each distinct line colour represents modal parameter curves generated through different fitting techniques. Specifically, first-order polynomials and smoothing splines have been used to fit the natural frequency data. Meanwhile, smoothing splines, cubic splines, and second-order polynomials have been utilised for modal damping and modal constant. FRF synthesis at 13 N is shown to emphasise the influence of the selected fitting method in Fig. 11b. The plotted FRF in the frequency range of 75–79 rad/s demonstrates that different curve-fitting approaches yield varying synthesis outcomes.

As mentioned in the previous sections, it should be noted that, for the present example, the synthesis of these FRFs inherently requires the evaluation of modal

parameters corresponding to response levels outside the range covered by the quasi-linear data. The purpose of this example is to study and show the limitations of the method. Consequently, extrapolation is a fundamental necessity when responses at lower levels need to be synthesised and has been applied in this example across all the evaluated fitting techniques to reconstruct the full frequency response.

The comparative analysis of various curve and spline fitting methods presented in this section demonstrates that while different approaches yield some variations in modal parameter curves (particularly in modal damping and constants), their impact on the receptance curve remains insignificant. However, supplementary studies omitted here for brevity indicate that extrapolating beyond experimental displacement levels can lead to severe deviations between estimated and actual FRF behaviours. This discrepancy is particularly pronounced in exact-fit spline methods (such as cubic spline) that force the curve through every data point, often introducing artificial geometries and high curvatures in the extrapolated regions. Consequently, when modal parameter extrapolation is required, polynomial fits or smoothing splines should be preferred over rigid interpolation techniques to prevent unnatural FRF distortions.

4 Experimental validation and verification of the FCT-HFS method

This section details the experimental validation of the proposed FCT-HFS method. Two benchmark structures from the literature, the length-modified Brake-Reuß beam (LBRB) and the Orion beam, are employed for validation of the proposed method. These configurations serve to evaluate the practical applicability and efficacy of the FCT-HFS method in realistic engineering structures. Here, it is important to note that force-controlled experiments for nonlinear systems may encounter some practical limitations. Standard control algorithms frequently yield poor results when the system response approaches an unstable branch of the FRC, often leading to jumps. In this study, the methodology is applied under the assumption that excitation force is effectively controlled, which is generally feasible within the response branches analysed here. Consequently, the methodology developed in this work is specifically designed for regions where jump phenomena do not occur.

4.1 Experimental case study 1: length modified Brake-Reuß beam

To validate the effectiveness of the FCT-HFS method, the results of the experiments performed on the length-modified Brake-Reuß beam [49] are utilised. The experimental setup, illustrated in Fig. 12, consists of two L-shaped stainless-steel beams rigidly connected via bolted joints tightened to 20 Nm. The assembled structure is subjected to a force-controlled stepped sine test using an electrodynamic shaker, targeting the first and second bending modes of the system. For this study, the data corresponding to the first bending mode are utilised. The experimental dataset is provided by the authors [49] per our request.

Figure 13a represents the reported FRCs of the force-controlled testing performed in [49], where the reported results of acceleration are converted to displacement amplitudes. Figure 13b and c show the harmonic force surface plot obtained from the data and the extracted quasi-linear FRFs, respectively. Smoothing spline curve fitting is applied to all identified modal parameters, as shown in Fig. 14. The results reveal some degree of response amplitude-dependent behaviour in the damping ratio as well as a softening type of non-linearity.

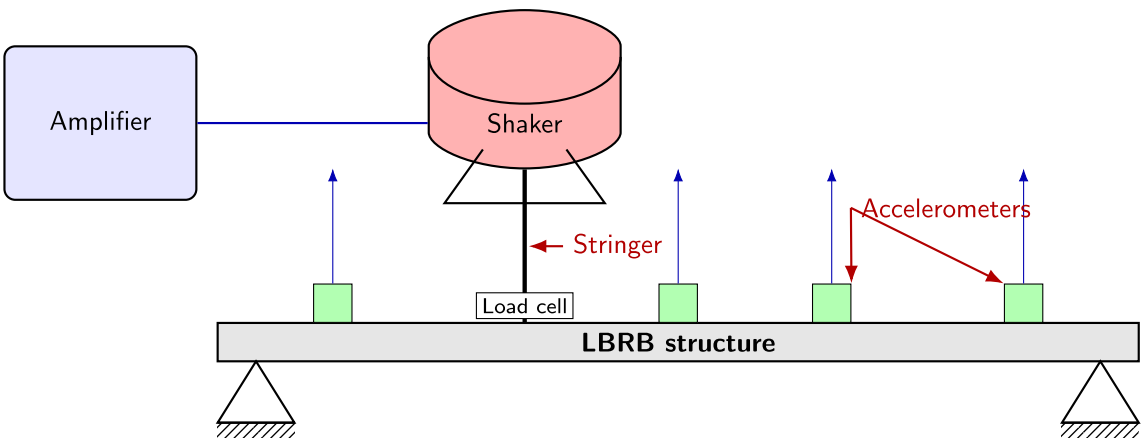

Fig. 12 Experimental setup for LBRB

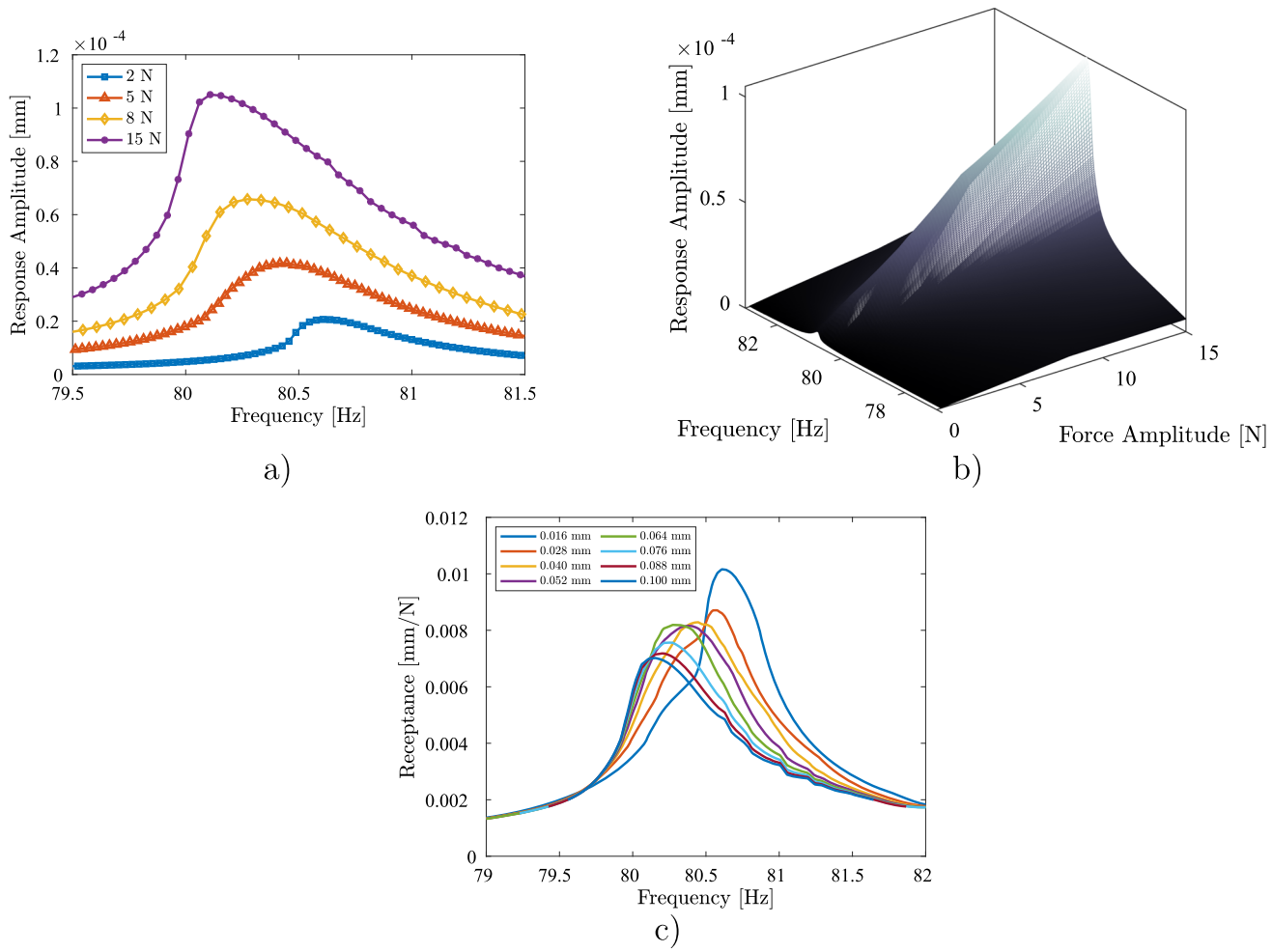

Fig. 13 **a** Measured FRCs, **b** The corresponding HFS, **c** Extracted quasi-linear FRFs, of the LBRB at the 1st mode

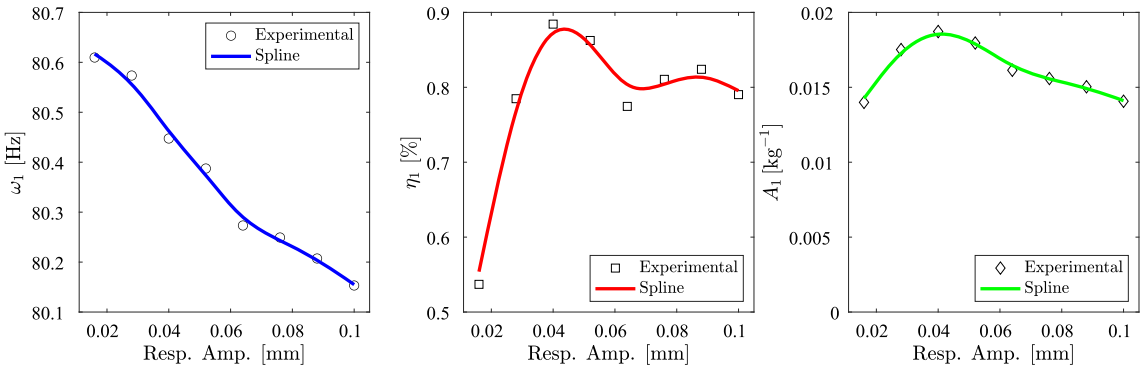

Fig. 14 Identified modal parameters for the LBRB at the 1st bending mode

Figure 15 compares the experimentally measured FRCs with those reconstructed using the identified modal parameters. The FCT-HFS method provides an accurate match near resonance frequencies (even more accurate match than [49]) for excitation levels of 2 N, 5 N, 8 N and a slightly increased mismatch is observed at the frequencies below resonance at the 15 N forcing level.

4.2 Experimental case study 2: the Orion beam

This case study examines the Orion beam [50] using the data set [51], a structure composed of two beams interconnected by three bolted joints. The experimental setup is illustrated in Fig. 16. In the test configuration, the beam is oriented vertically, with its neutral axis perpendicular to

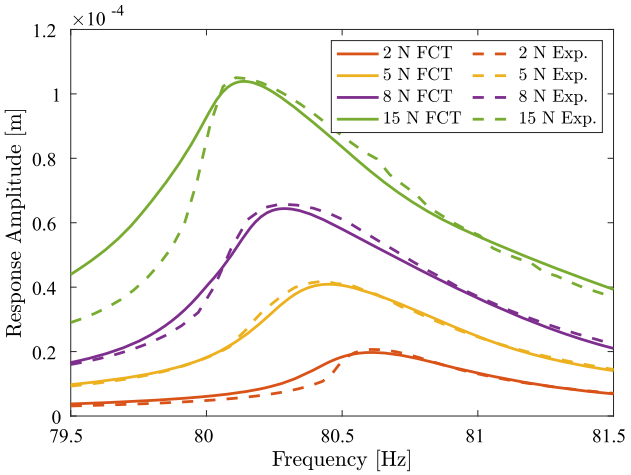

Fig. 15 FRCs comparison for the LBRB at the 1st bending mode

the ground to minimise the influence of gravitational forces and to suppress torsional vibration modes. To investigate the impact of design parameters on experimental repeatability, variations in both the bolt tightening torques and the excitation force are introduced. A feedback control system enables force-controlled testing around the beam's third and sixth bending mode frequencies.

4.2.1 Third bending mode

The experimental analysis of the third bending mode covers the 280–300 Hz frequency range, with a frequency resolution of 0.3906 Hz. These tests are performed at a bolted joint tightening torque of 20 and 80 cNm under five distinct forcing levels: 10, 50, 100, 150, and 200 mN. While the FCT-HFS method has been previously applied to the 20 cNm data set by Gürbüz et al. [42], this study focuses on the higher torque level (80 cNm).

The results are presented in Fig. 17, which illustrates (a) the experimentally measured FRCs, (b) the corresponding HFS, and (c) the extracted quasi-linear FRFs. Modal parameters (natural frequency, modal damping, and modal constant) are identified from the quasi-linear FRFs. To enhance interpretability, curve fitting is applied to these parameters: a quadratic polynomial fit for the natural frequency and the modal constant, and a spline fit for the modal damping ratio, as shown in Fig. 18. The damping characteristics reveal a significant level of nonlinearity; notably, the modal damping ratio at the peak response amplitude exceeds that value at the lowest amplitude by a factor exceeding three.

Finally, the measured FRFs and the synthesised FRFs, obtained via the identified modal parameters, are compared in Fig. 19. The results demonstrate a high degree of correlation between the measured and synthesised responses, validating the effectiveness of the FCT-HFS method in accurately capturing the nonlinear dynamic behaviour of the beam in the third bending mode.

4.2.2 Sixth bending mode

To further assess the robustness of the proposed FCT-HFS method, experimental data around the sixth bending mode of the Orion beam are utilised. In [50], experiments encompass five bolt tightening torque levels (10, 20, 30, 80, and 1000 cNm, the latter representing a glued joint) with excitation forces ranging from 10 to 250 mN. For the sake of brevity, only a representative dataset corresponding to the 1000 cNm (glued) case is presented here.

Figure 20 displays (a) the measured FRCs, (b) the corresponding HFS, and (c) the extracted quasi-linear FRFs. In this study, the modal parameters for the analysis around the sixth bending mode of the Orion beam are identified using the peak-picking method. Subsequently, a first-order polynomial is employed to model the natural frequency, while spline curve fitting is used for the modal damping ratio and modal constant, as illustrated in Fig. 21. It can be

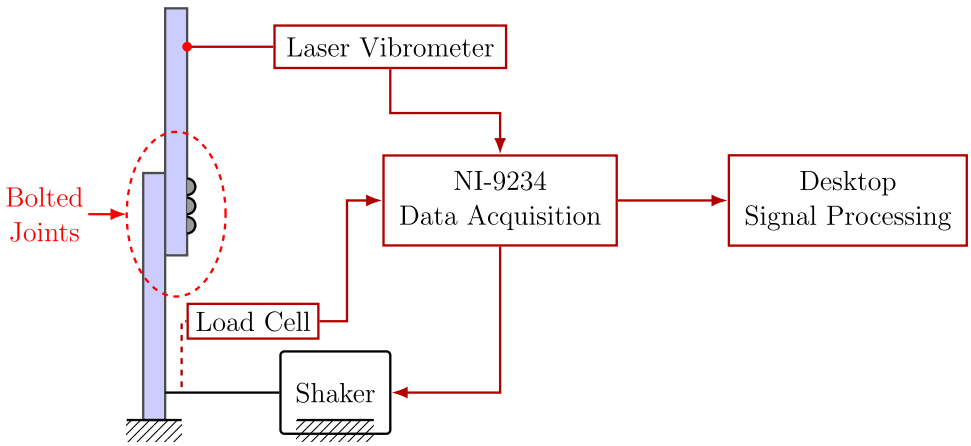

Fig. 16 Schematic Representation of the beam

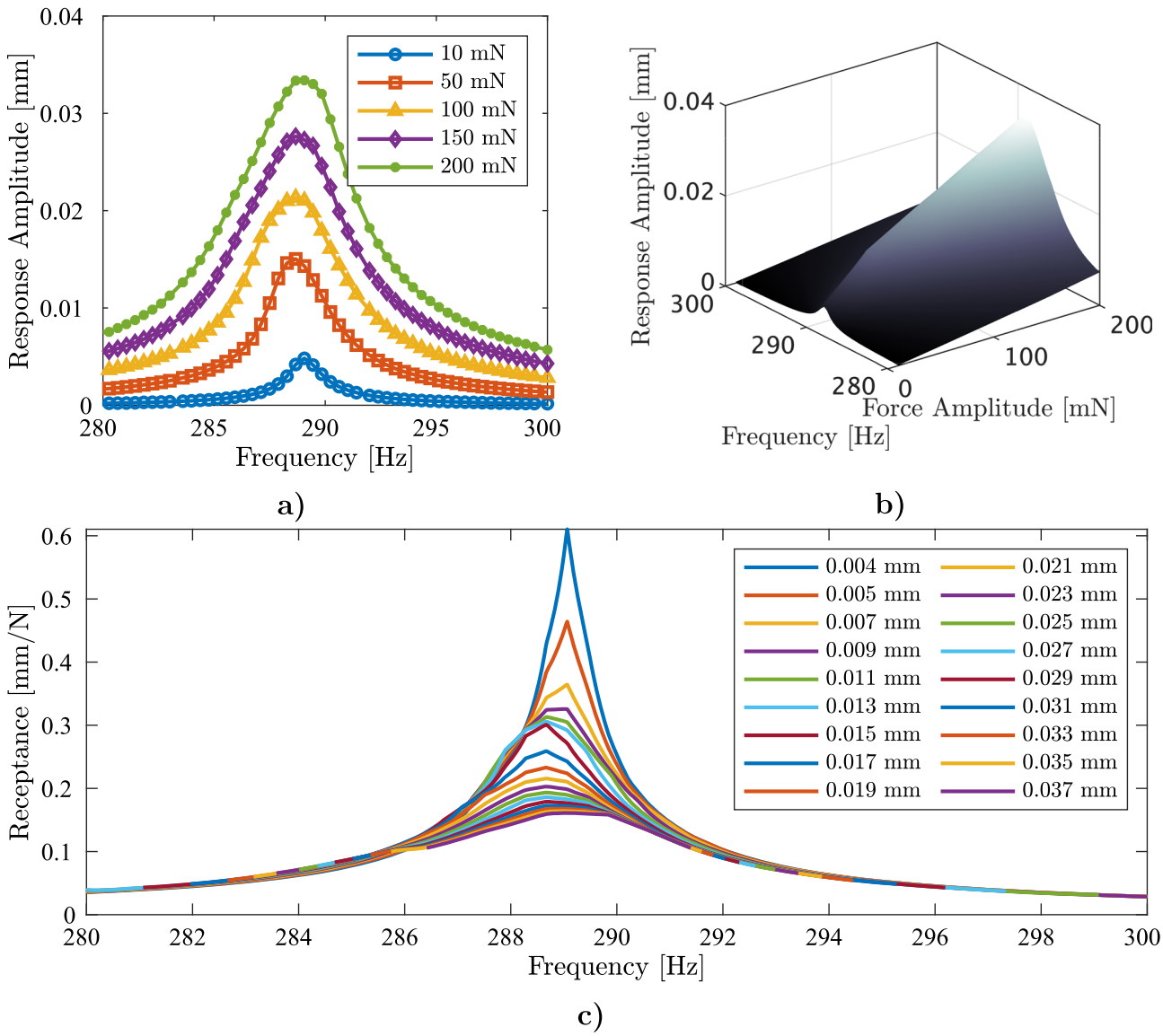

Fig. 17 **a** Measured FRCs, **b** The corresponding HFS, **c** Extracted quasi-linear FRFs, of the Orion beam at the 3rd bending mode

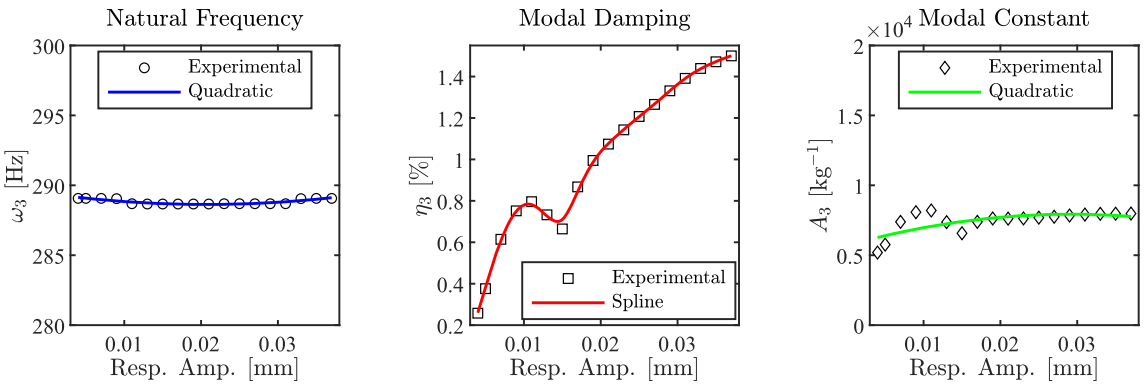

Fig. 18 Identified modal parameters for the Orion beam at the 3rd bending mode

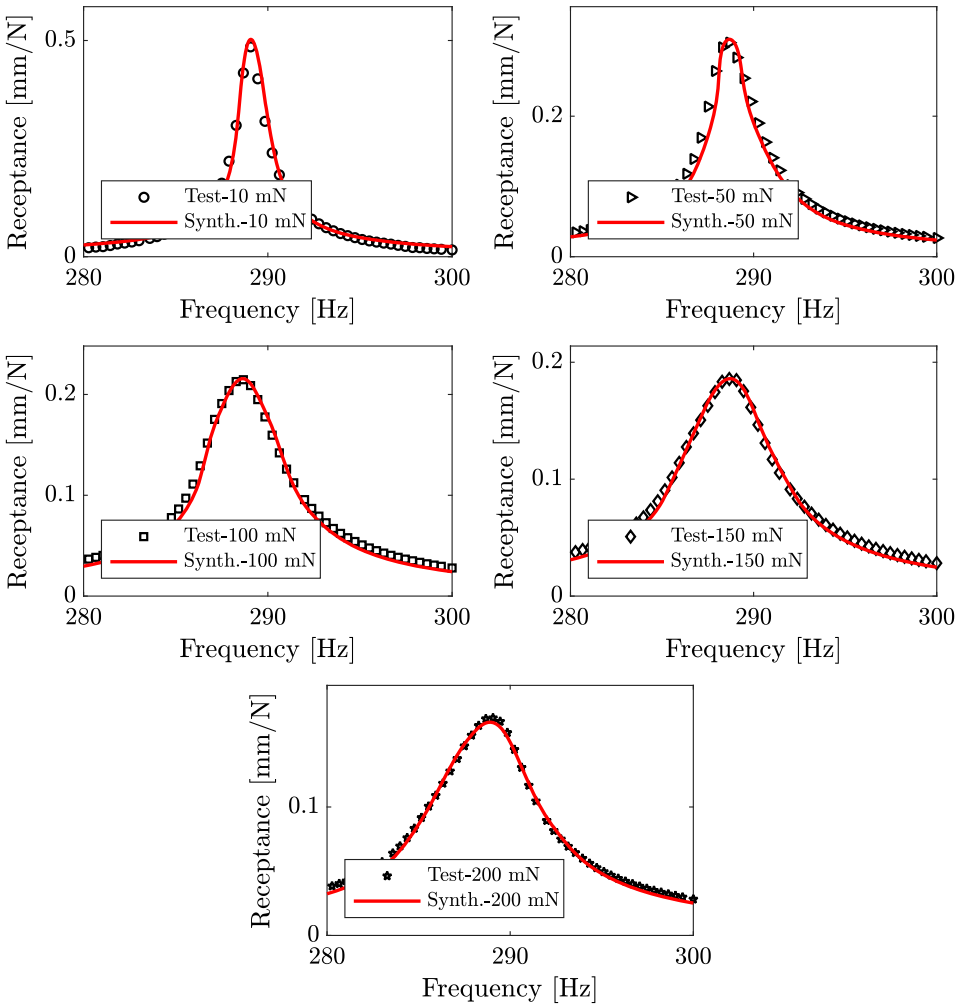

Fig. 19 FRFs comparison for the Orion beam at the 3rd bending mode

observed that the modal parameters exhibit a mild variation with respect to response amplitude.

A comparison between the experimentally measured FRFs and those synthesised using the identified and fitted modal parameters is shown in Fig. 22. A strong correlation is observed across most forcing levels. A slight deviation noted at the lowest excitation level (10 mN) is attributed to limitations in the HFS construction. At lower response amplitude levels, quasi-linear FRFs might not be available to slice from the HFS. Therefore, this causes the need for inevitable extrapolation for the lower response amplitude levels, creating deviations from the original FRCs.

5 Conclusion

This paper introduces a novel approach for obtaining modal models of nonlinear systems using classical force-controlled stepped-sine testing. The proposed FCT-HFS method is applicable to systems with many nonlinearities, regardless of their types and locations, provided that the modes of the system are sufficiently separated and no internal resonances are present.

To apply the method, force-controlled sine tests are conducted for several force values to generate an HFS, which is a three-dimensional surface formed by merging measured frequency response curves along the force amplitude axis, an additional orthogonal axis to the frequency and response amplitude plane. The HFS is subsequently sliced by multiple constant response amplitude planes to extract harmonic force spectra, from which quasi-linear FRFs, each corresponding to a different response amplitude, are indirectly determined. Modal parameters are then identified for each response amplitude level of the nonlinear system, employing the quasi-linear FRFs. These identified amplitude-dependent modal parameters constitute the modal model of the nonlinear system, the validity of which is then demonstrated by reconstructing the FRCs and comparing them with the original ones.

The proposed approach is validated through both numerical simulations and experimental investigations. In the simulated case studies, a discrete system with cubic

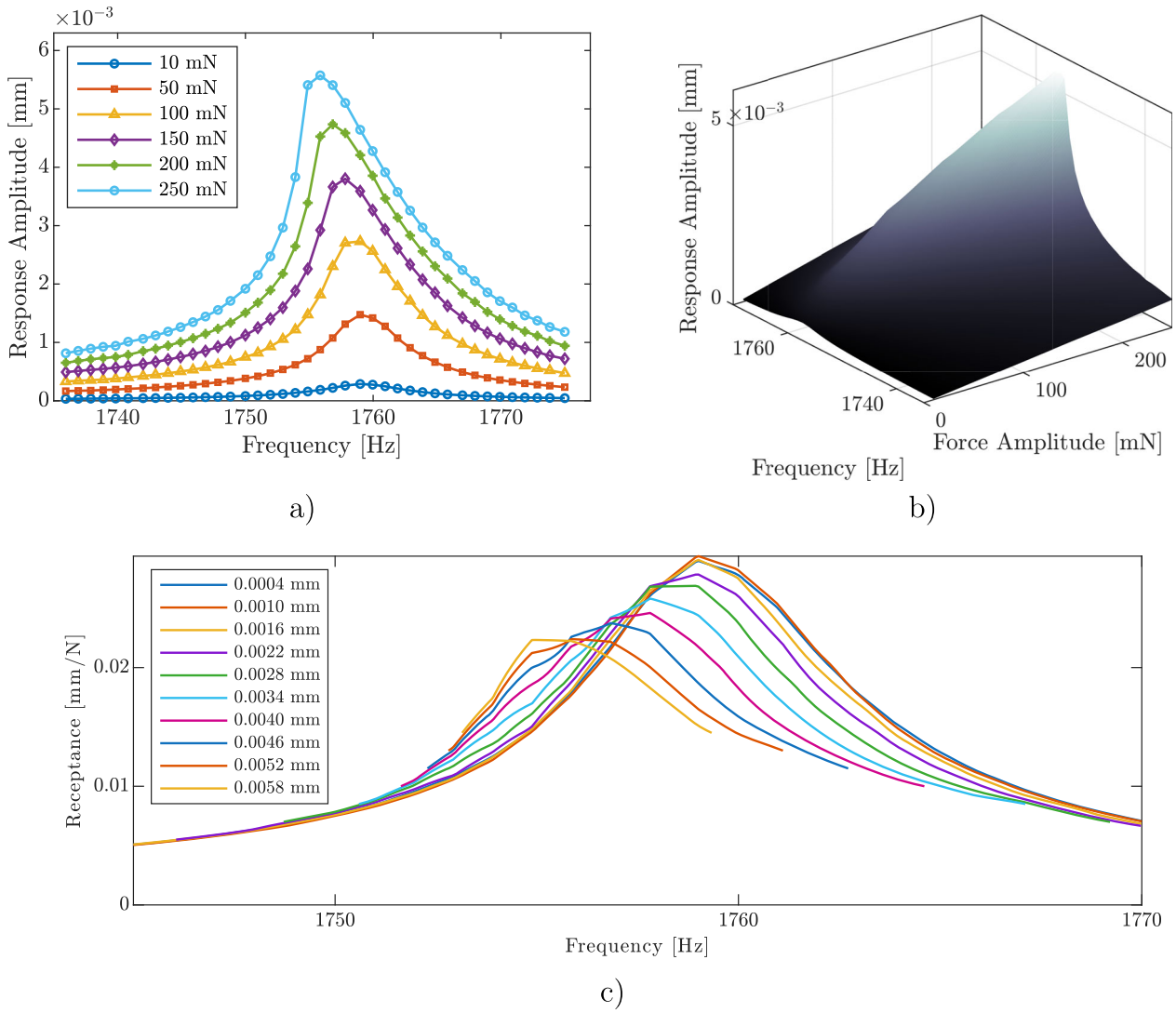

Fig. 20 **a** Measured FRCs, **b** The corresponding HFS, **c** Extracted quasi-linear FRFs, of the Orion beam at the 6th bending mode

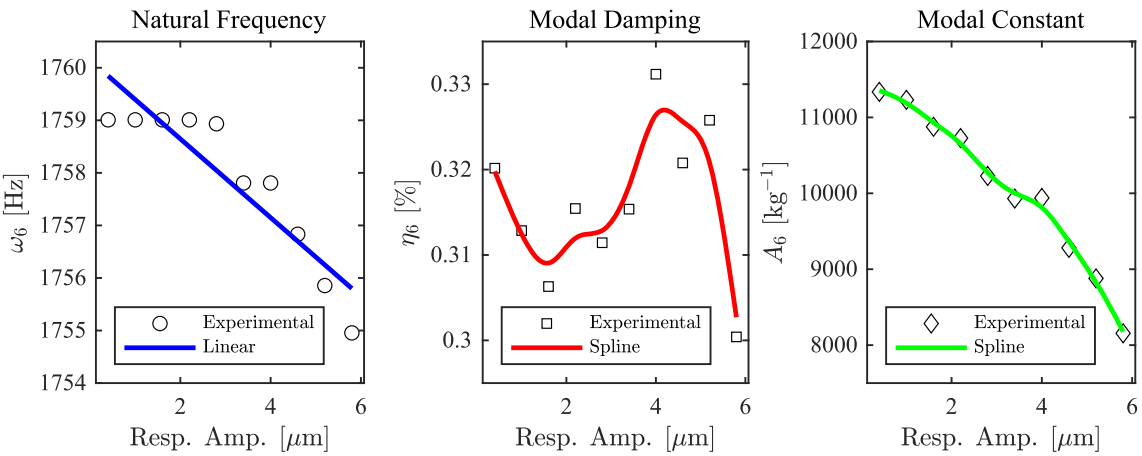

Fig. 21 Identified modal parameters for the Orion beam at the 6th bending mode

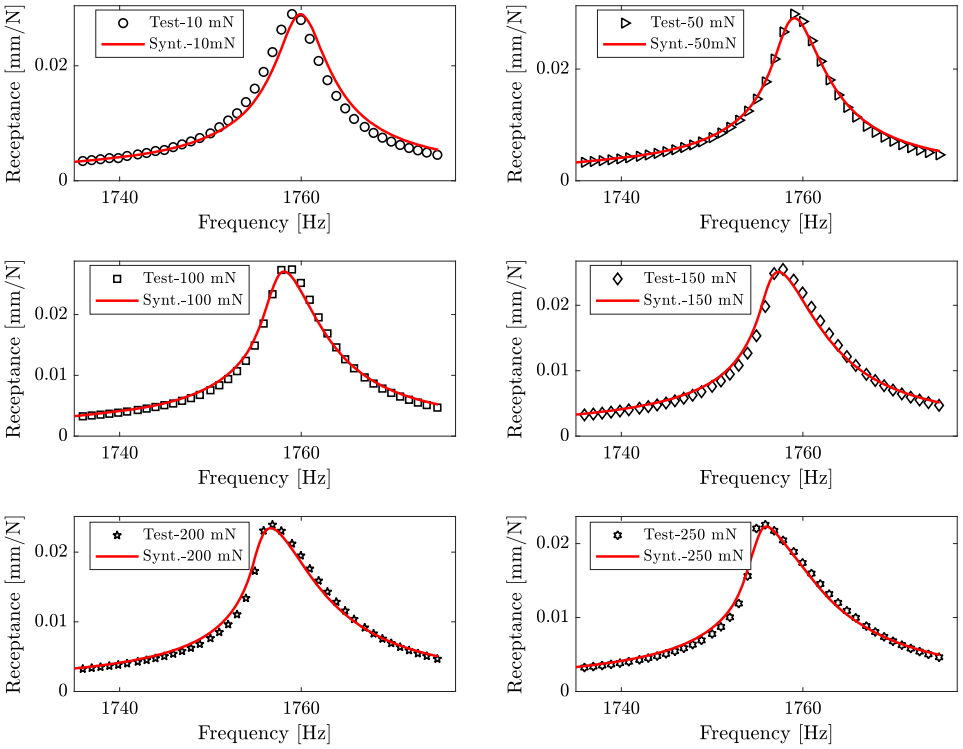

Fig. 22 FRFs comparison for the Orion beam at the 6th bending mode

stiffness nonlinearity is used, whereas in the experimental validation, three experimental benchmark system datasets from the literature are used.

The observations made and the conclusions reached in this study can be summarised as follows:

1. When the nonlinearity is weak, so that there is no jump in the frequency response, the FCT-HFS approach is very successful in obtaining a nonlinear modal model.
2. When there is a stronger nonlinearity that introduces a jump, causing an unstable branch in the FRC, it leads to partially distorted quasi-linear FRFs or an incomplete quasi-linear FRF, which cannot be directly used for modal identification. It is then proposed to utilise the undistorted/complete part of the quasi-linear FRF to identify amplitude-dependent modal parameters, assuming symmetry about the resonance frequency within the half-power point bandwidth. This approach ensures that the approximation remains consistent with quasilinear FRFs and yields reasonable accuracy in the synthesised FRFs for the case studied here. The applicability of this approach is shown with a numerical simulation case study in Sect. 3.
3. The proposed method can be used for strongly nonlinear systems if the nonlinearity is due to damping, provided that there is no jump in the frequency response, e.g. in the case of friction nonlinearity. Thus, it can be concluded that the method performs more effectively for nonlinear systems which do not cause unstable branches.
4. Conducting a sufficient number of tests in the construction of the HFS is critical, as it yields more accurate quasi-linear FRFs and more accurate identified modal parameters.
5. The selection of the curve-fitting technique for modal parameters is important, as it directly influences the accuracy and reliability of the subsequent synthesis process. When extrapolation is necessary because experimental data are unavailable, it should be performed with caution, and spline-fitting methods that impose artificial or physically unjustified curvature should be avoided.

Despite some challenges and limitations of the proposed FCT-HFS framework, the primary advantage of it lies in its ability to use classical force-controlled tests, which are well-established and widely used within both industrial and academic settings, and thus to avoid tests that require complex controllers to be designed, as response-controlled testing is only achieved successfully with a specific commercial controller. Many legacy test systems are not capable of performing reliable response-controlled measurements without externally designed and implemented controllers, which may not always achieve comparable performance [36]. Moreover, as the accuracy of the synthesised FRCs inherently depends on the curve-fitting applied to the HFS cross-sections, a dedicated future study

investigating the optimal bounds and sampling density of the selected displacement range and force is recommended. Future work may explore the feasibility of constructing an HFS within the proposed framework using the frequency, force, and response data obtained through either FFVCT or fixed-voltage frequency sweeps conducted at several voltage levels. For both approaches, the resulting HFS coverage and the effects of shaker-structure interaction, back-EMF, and higher harmonic content should be investigated.

Acknowledgements M. Fatih Gürbüz acknowledges the fellowship of the Ministry of National Education of the Republic of Türkiye. The authors acknowledge Dr. Sina Safari for providing the data set from their work.

Author contributions M. Fatih Gürbüz: Conceptualisation, Methodology, Software, Validation, Investigation, Writing—original draft. M. Bülent Özer: Supervision, Conceptualisation, Methodology, Writing—review and editing. H. Nevzat Özgüven: Supervision, Conceptualisation, Methodology, Writing—review and editing.

Funding This work received no funding.

Data availability We synthetically generated our numerical example data to validate and test the method. For the experimental case we used open access data for the Orion beam to validate the method. And requested the experimental data from authors for the LBRB experimental case study and used their experimental data.

Declarations

Conflict of interest The authors declare that they have no conflict of interest.

Open Access This article is licensed under a Creative Commons Attribution 4.0 International License, which permits use, sharing, adaptation, distribution and reproduction in any medium or format, as long as you give appropriate credit to the original author(s) and the source, provide a link to the Creative Commons licence, and indicate if changes were made. The images or other third party material in this article are included in the article's Creative Commons licence, unless indicated otherwise in a credit line to the material. If material is not included in the article's Creative Commons licence and your intended use is not permitted by statutory regulation or exceeds the permitted use, you will need to obtain permission directly from the copyright holder. To view a copy of this licence, visit http://creativecommons.org/licenses/by/4.0/.

References

1. Ljung, L.: System Identification: Theory for the User. Prentice-Hall (1986)
2. Kerschen, G., Worden, K., Vakakis, A.F., Golinval, J.-C.: Past, present and future of nonlinear system identification in structural dynamics. Mech. Syst. Signal Process. **20**, 505–592 (2006). https://doi.org/10.1016/j.ymssp.2005.04.008
3. Noël, J.P., Kerschen, G.: Nonlinear system identification in structural dynamics: 10 more years of progress. Mech. Syst. Signal Process. **83**, 2–35 (2017). https://doi.org/10.1016/j.ymssp.2016.07.020
4. Rosenberg, R.M.: Normal modes of nonlinear dual-mode systems. J. Appl. Mech. **27**, 263–268 (1960). https://doi.org/10.1115/1.3643948
5. Rosenberg, R.M.: The normal modes of nonlinear n-degree-of-freedom systems. J. Appl. Mech. **29**, 7–14 (1962). https://doi.org/10.1115/1.3636501
6. Rosenberg, R.M.: On nonlinear vibrations of systems with many degrees of freedom. In: Advances in Applied Mechanics, pp. 155–242. Elsevier (1966). https://doi.org/10.1016/S0065-2156(08)70008-5
7. Szemplińska-Stupnicka, W.: The modified single mode method in the investigations of the resonant vibrations of non-linear systems. J. Sound Vib. **63**, 475–489 (1979). https://doi.org/10.1016/0022-460X(79)90823-X
8. Szemplinska-Stupnicka, W.: "Non-linear normal modes" and the generalized Ritz method in the problems of vibrations of nonlinear elastic continuous systems. Int. J. Non-Linear Mech. **18**, 149–165 (1983). https://doi.org/10.1016/0020-7462(83)90042-2
9. Jézéquel, L.: Structural damping by slip in joints. J. Vib. Acoust. **105**, 497–504 (1983). https://doi.org/10.1115/1.3269134
10. Setio, S., Setio, H.D., Jezequel, L.: A method of non-linear modal identification from frequency response tests. J. Sound Vib. **158**, 497–515 (1992). https://doi.org/10.1016/0022-460X(92)90421-S
11. Chong, Y.H., Imregun, M.: Development and application of a nonlinear modal analysis technique for MDOF systems. J. Vib. Control **7**, 167–179 (2001). https://doi.org/10.1177/107754630100700202
12. Gibert, C.: Fitting measured frequency response using non-linear modes. Mech. Syst. Signal Process. **17**, 211–218 (2003). https://doi.org/10.1006/mssp.2002.1562
13. Platten, M.F., Wright, J.R., Dimitriadis, G., Cooper, J.E.: Identification of multi-degree of freedom non-linear systems using an extended modal space model. Mech. Syst. Signal Process. **23**, 8–29 (2009). https://doi.org/10.1016/j.ymssp.2007.11.016
14. Platten, M.F., Wright, J.R., Dimitriadis, G., Cooper, J.E.: Identification of a nonlinear wing structure using an extended modal model. J. Aircr. **46**, 1614–1626 (2009). https://doi.org/10.2514/1.42024
15. Fuellekrug, U., Goege, D.: Identification of weak non-linearities within complex aerospace structures. Aerosp. Sci. Technol. **23**, 53–62 (2012). https://doi.org/10.1016/j.ast.2011.04.012
16. Özer, M.B., Özgüven, H.N., Royston, T.J.: Identification of structural non-linearities using describing functions and the Sherman-Morrison method. Mech. Syst. Signal Process. **23**, 30–44 (2009). https://doi.org/10.1016/j.ymssp.2007.11.014
17. Aykan, M., Nevzat Özgüven, H.: Parametric identification of nonlinearity in structural systems using describing function inversion. Mech. Syst. Signal Process. **40**, 356–376 (2013). https://doi.org/10.1016/j.ymssp.2013.03.016
18. Ahmadian, H., Jalali, H., Pourahmadian, F.: Nonlinear model identification of a frictional contact support. Mech. Syst. Signal Process. **24**, 2844–2854 (2010). https://doi.org/10.1016/j.ymssp.2010.06.007
19. Masri, S.F., Caughey, T.K.: A nonparametric identification technique for nonlinear dynamic problems. J. Appl. Mech. **46**, 433–447 (1979). https://doi.org/10.1115/1.3424568
20. Wang, X., Zheng, G.T.: Equivalent dynamic stiffness mapping technique for identifying nonlinear structural elements from frequency response functions. Mech. Syst. Signal Process. **68–69**, 394–415 (2016). https://doi.org/10.1016/j.ymssp.2015.07.011
21. Sracic, M.W., Allen, M.S.: Method for identifying models of nonlinear systems using linear time periodic approximations. Mech. Syst. Signal Process. **25**, 2705–2721 (2011). https://doi.org/10.1016/j.ymssp.2011.03.004
22. Noël, J.P., Kerschen, G.: Frequency-domain subspace identification for nonlinear mechanical systems. Mech. Syst. Signal

Process. **40**, 701–717 (2013). https://doi.org/10.1016/j.ymssp.2013.06.034
23. delli Carri, A., Ewins, D.J.: Nonlinear identification of a numerical benchmark structure: from measurements to FE model updating. In: International Seminar on Modal Analysis (ISMA), pp. Leuven, Belgium (2014)
24. Kwarta, M., Allen, M.S.: Nonlinear identification through eXtended outputs (NIXO) with numerical and experimental validation using geometrically nonlinear structures. Mech. Syst. Signal Process. **200**, 110542 (2023). https://doi.org/10.1016/j.ymssp.2023.110542
25. Adams, D.E., Allemang, R.J.: A frequency domain method for estimating the parameters of a nonlinear structural dynamic model through feedback. Mech. Syst. Signal Process. **14**, 637–656 (2000). https://doi.org/10.1006/mssp.2000.1292
26. Renson, L., Gonzalez-Buelga, A., Barton, D.A.W., Neild, S.A.: Robust identification of backbone curves using control-based continuation. J. Sound Vib. **367**, 145–158 (2016). https://doi.org/10.1016/j.jsv.2015.12.035
27. Peter, S., Leine, R.I.: Excitation power quantities in phase resonance testing of nonlinear systems with phase-locked-loop excitation. Mech. Syst. Signal Process. **96**, 139–158 (2017). https://doi.org/10.1016/j.ymssp.2017.04.011
28. Karaağaçlı, T., Özgüven, H.N.: Experimental modal analysis of nonlinear systems by using response-controlled stepped-sine testing. Mech. Syst. Signal Process. **146**, 107023 (2021). https://doi.org/10.1016/j.ymssp.2020.107023
29. Arslan, Ö., Özgüven, H.N.: Modal identification of non-linear structures and the use of modal model in structural dynamic analysis. In: 26th International Modal Analysis Conference IMAC, pp. Orlando (2008)
30. Arslan, Ö., Aykan, M., Nevzat Özgüven, H.: Parametric identification of structural nonlinearities from measured frequency response data. Mech. Syst. Signal Process. **25**, 1112–1125 (2011). https://doi.org/10.1016/j.ymssp.2010.10.010
31. Karaağaçlı, T., Özgüven, H.N.: Experimental quantification and validation of modal properties of geometrically nonlinear structures by using response-controlled stepped-sine testing. Exp. Mech. **62**, 199–211 (2022). https://doi.org/10.1007/s11340-021-00784-9
32. Karaağaçlı, T., Özgüven, H.N.: Experimental modal analysis of geometrically nonlinear structures by using response-controlled stepped-sine testing. In: Nonlinear Structures and Systems, vol. 1, pp. 123–134. Springer International Publishing Cham (2022)
33. Koyuncu, A., Karaağaçlı, T., Şahin, M., Özgüven, H.N.: Experimental modal analysis of nonlinear amplified piezoelectric actuators by using response-controlled stepped-sine testing. Exp. Mech. **62**, 1579–1594 (2022). https://doi.org/10.1007/s11340-022-00878-y
34. Karaağaçlı, T., Nevzat Özgüven, H.: Experimental modal analysis of structures with high nonlinear damping by using response-controlled stepped-sine testing. In: Nonlinear Structures and Systems, vol. 1, pp. 125–132. Springer Nature Switzerland Cham (2024)
35. Karaağaçlı, T., Özgüven, H.N.: Experimental identification of backbone curves of strongly nonlinear systems by using response-controlled stepped-sine testing (RCT). Vibration **3**, 266–280 (2020). https://doi.org/10.3390/vibration3030019
36. Arati Bhattu, S.H., Jamia, N., Müller, F., Scheel, M., Schwingshackl, C., Nevzat Özgüven, H., Krack, M.: Experimental analysis of the TRC benchmark system. J. Struct. Dyn. (2024). https://doi.org/10.25518/2684-6500.206
37. Maio, D.D.: A novel analysis method for calculating nonlinear Frequency Response Functions. J. Struct. Dyn. (2025). https://doi.org/10.25518/2684-6500.242
38. Karaağaçlı, T., Özgüven, H.N.: A frequency domain nonparametric identification method for nonlinear structures: describing surface method. Mech. Syst. Signal Process. **144**, 106872 (2020). https://doi.org/10.1016/j.ymssp.2020.106872
39. Zhang, G., Zang, C., Friswell, M.I.: Measurement of multivalued response curves of a strongly nonlinear system by exploiting exciter dynamics. Mech. Syst. Signal Process. **140**, 106474 (2020). https://doi.org/10.1016/j.ymssp.2019.106474
40. Zhang, G., Zang, C., Friswell, M.I.: Parameter identification of a strongly nonlinear rotor-bearing system based on reconstructed constant response tests. J. Eng. Gas Turbines Power (2020). https://doi.org/10.1115/1.4047783
41. Robbins, E., Kuether, R.J., Pacini, B.R., Moreu, F.: Stabilizing a strongly nonlinear structure through shaker dynamics in fixed frequency voltage control tests. Mech. Syst. Signal Process. **190**, 110118 (2023). https://doi.org/10.1016/j.ymssp.2023.110118
42. Gürbüz, M.F., Karaağaçlı, T., Özer, M.B., Özgüven, H.N.: Bypassing the repeatability issue in nonlinear experimental modal analysis of jointed structures by using the RCT-HFS framework. In: Nonlinear Structures and Systems, vol. 1, pp. 75–80. Springer Nature Switzerland Cham (2024)
43. Gürbüz, M.F.: Obtaining modal models of a nonlinear structure using force-controlled frequency response functions. Middle East Technical University, Ankara (2024)
44. Tanrikulu, O., Kuran, B., Ozguven, H.N., Imregun, M.: Forced harmonic response analysis of nonlinear structures using describing functions. AIAA J. **31**, 1313–1320 (1993). https://doi.org/10.2514/3.11769
45. Budak, E., Nevzat Özgüven, H.: Iterative receptance method for determining harmonic response of structures with symmetrical non-linearities. Mech. Syst. Signal Process. **7**, 75–87 (1993). https://doi.org/10.1016/0888-3270(93)90006-I
46. Kuran, B., Özgüven, H.N.: A modal superposition method for nonlinear structures. J. Sound Vib. **189**, 315–339 (1996). https://doi.org/10.1006/jsvi.1996.0022
47. Ferhatoglu, E., Cigeroglu, E., Özgüven, H.N.: A novel modal superposition method with response dependent nonlinear modes for periodic vibration analysis of large MDOF nonlinear systems. Mech. Syst. Signal Process. **135**, 106388 (2020). https://doi.org/10.1016/j.ymssp.2019.106388
48. Ferhatoglu, E., Groß, J., Krack, M.: Frequency response variability in friction-damped structures due to non-unique residual tractions: obtaining conservative bounds using a nonlinear-mode-based approach. Mech. Syst. Signal Process. **201**, 110651 (2023). https://doi.org/10.1016/j.ymssp.2023.110651
49. Safari, S., Londoño Monsalve, J.M.: Data-driven structural identification of nonlinear assemblies: structures with bolted joints. Mech. Syst. Signal Process. **195**, 110296 (2023). https://doi.org/10.1016/j.ymssp.2023.110296
50. Teloli, R.O., Butaud, P., Chevallie, G., da Silva, S.: Good practices for designing and experimental testing of dynamically excited jointed structures: the Orion beam. Mech. Syst. Signal Process. **163**, 108172 (2022). https://doi.org/10.1016/j.ymssp.2021.108172
51. Teloli, R.O., Butaud, P., Chevallier, G., da Silva, S.: Dataset of experimental measurements for the Orion beam structure. Data Brief **39**, 107627 (2021). https://doi.org/10.1016/j.dib.2021.107627

Publisher's Note Springer Nature remains neutral with regard to jurisdictional claims in published maps and institutional affiliations.